INACTIVATION MECHANISM OF POLYPHENOL OXIDASE
DURING ULTRASOUND TREATMENT

A THESIS SUBMITTED TO
THE GRADUATE SCHOOL OF NATURAL AND APPLIED SCIENCES
OF
MIDDLE EAST TECHNICAL UNIVERSITY

BY

HANDE BALTACIOĞLU

IN PARTIAL FULFILLMENT OF THE REQUIREMENTS
FOR
THE DEGREE OF DOCTOR OF PHILOSOPHY
IN
FOOD ENGINEERING

JUNE 2014

Approval of the thesis:

INACTIVATION MECHANISM OF POLYPHENOL OXIDASE DURING ULTRASOUND TREATMENT

submitted by **HANDE BALTACIOĞLU** in partial fulfillment of the requirements for the degree of **Doctor of Philosophy in Food Engineering Department, Middle East Technical University** by,

Prof. Dr. Canan Özgen   _____
Dean, Graduate School of **Natural and Applied Sciences**

Prof. Dr. Alev Bayındırlı   _____
Head of Department, **Food Engineering**

Prof. Dr. Alev Bayındırlı   _____
Supervisor, **Food Engineering Dept., METU**

Prof. Dr. Feride Severcan   _____
Co-Supervisor, **Biological Sciences Dept., METU**

Examining Committee Members:

Prof. Dr. Hami Alpas   _____
Food Engineering Dept., METU

Prof. Dr. Alev Bayındırlı   _____
Food Engineering Dept., METU

Prof. Dr. Vural Gökmen   _____
Food Engineering Dept., Hacettepe University

Assist. Prof. Dr. İlkay Şensoy   _____
Food Engineering Dept., METU

Assist. Prof. Dr. H. Mecit Öztop   _____
Food Engineering Dept., METU

Date: 03.06.2014

I hereby declare that all information in this document has been obtained and presented in accordance with academic rules and ethical conduct. I also declare that, as required by these rules and conduct, I have fully cited and referenced all material and results that are not original to this work.

Name, Last name: Hande Baltacıoğlu

Signature:

ABSTRACT

INACTIVATION MECHANISM OF POLYPHENOL OXIDASE
DURING ULTRASOUND TREATMENT

BALTACIOĞLU, Hande

Ph. D., Department of Food Engineering

Supervisor: Prof. Dr. Alev BAYINDIRLI

Co-Supervisor: Prof. Dr. Feride SEVERCAN

June 2014, 109 pages

In this study, the activity and conformational changes of mushroom polyphenol oxidase (PPO) were investigated during the inactivation by heat-ultrasound treatment at different power, temperature and time combinations. The secondary structure change of the enzyme during inactivation was analyzed by using Fourier Transform Infrared (FTIR) spectroscopy and compared with the enzyme activity change.

In thermosonication (TS) treatment, the residual enzyme activity decreased with increasing power, time and temperature. The enzyme inactivation higher than 99 % was obtained at 100 % amplitude at 60 °C for 10 min. For comparison, when the stability of mushroom PPO after thermal treatment was investigated, approximately 99% inactivation was obtained at 70 °C for 5 min. D value for thermal treatment at 60°C was found as 6.66 min whereas for 100, 80 and 60 % amplitude TS treatments at the same temperature, D values were found as 2.09, 3.33 and 3.44 min, respectively.

FTIR studies showed that the thermal and TS treatments caused an irreversible change on the secondary structure of the enzyme. α-helix and β-sheet content decreased, while aggregated β-sheet, turns and random coil content increased during the temperature increase. The transition temperature (T_m) values of TS and thermal treatments were 44 and 55 ºC, respectively. This result showed that heat and ultrasound combination behaved synergistically on the conformational change of the enzyme. Compared to the thermal treatment, TS treatment seemed to be more effective on the secondary structural change at lower temperatures.

Keywords: Polyphenol oxidase, enzyme inactivation, ultrasound, Fourier Transform Infrared spectroscopy, protein secondary structure.

ÖZ

ULTRASON UYGULAMASINDA POLİFENOL OKSİDAZ ENZİMİNİN İNAKTİVASYON MEKANİZMALARI

BALTACIOĞLU, Hande

Doktora, Gıda Mühendisliği Bölümü

Tez Yöneticisi: Prof. Dr. Alev BAYINDIRLI

Ortak Tez Yöneticisi: Prof. Dr. Feride SEVERCAN

Haziran 2014, 109 sayfa

Bu araştırmada farklı güç, sıcaklık ve süre etkileri göz önüne alınarak, ısı-ultrason kombinasyonu inaktivasyonu sonrasında mantar PPO enziminin aktivite ve yapısal değişimleri incelenmiştir. İnaktivasyon boyunca enzimin ikincil yapısındaki değişiklikler, Fourier Dönüşüm Kızıl Ötesi (FTIR) spektroskopisi kullanılarak analiz edilmiş ve bu sonuçlar aktivitedeki değişiklikler ile karşılaştırılmıştır.

Termosonikasyon (TS) uygulamasında artan sıcaklık, zaman ve genlik ile enzim aktivitesinin azaldığı belirlenmistir. %100 genlikte, 60 °C' de 10 dakika TS uygulaması ile % 99` dan fazla inaktivasyon elde edilmiştir. Kıyaslama için ısıl işlem uygulaması sonrasında enzim aktivitesi belirlenmiş ve 70 °C de 5 dakika sonunda yaklaşık % 99 oranında inaktivasyon elde edilmiştir D_{60} değeri ısıl işlem için 6.66 dakika, % 100, 80 ve 60 genlik TS uygulaması için sırasıyla 2.09, 3.33 ve 3.44 olarak bulunmuştur.

FTIR çalışmaları, uygulanan ısıl işlem ve termosonikasyonun enzimin ikincil yapısı üzerinde geri dönüşümsüz bir inaktivasyona neden olduğunu ve ısıl işlem ve TS boyunca artan sıcaklık ile α-sarmal ve β-tabaka yapı içeriğinin azalırken, toplanmış β-tabaka yapı, dönüşler ve tesadüfi kıvrımlar içeriğinin arttığını göstermektedir. Geçiş sıcaklık değeri (T_m), TS ve ısıl işlem için sırasıyla 44 ve 55 °C olarak bulunmuştur. Bu sonuçlar, ısı ve ultrason kombinasyonunun enzimin yapısal değişiklikleri üzerine sinerjetik etkisi olduğunu göstermektedir. Isıl işlem ile karşılaştırıldığında, TS uygulamasının düşük sıcaklıklarda ikincil yapı değişiklikleri üzerine daha etkili olduğu görülmektedir.

Anahtar Kelimeler: Polifenol oksidaz, enzim inaktivasyonu, ultrason, Fourier Değişim Kızıl Ötesi spektroskopisi, protein ikincil yapısı.

"To my father"

ACKNOWLEDGEMENTS

Finally, I would like to express my deepest gratitude to my family, my husband and the best friend in my life Dr. Cem Baltacıoğlu, my daughter Ece Baltacıoğlu and my son Emre Baltacıoğlu for their love, endless patience and encouragement. Any word is not enough to express my appreciation to them. With love I dedicate this work to them.

TABLE OF CONTENTS

LIST OF TABLES

TABLES

LIST OF FIGURES

LIST OF SYMBOLS AND ABBREVIATIONS

BSA   Bovine Serum Albumin

CD   Circular Dichroism

FA   Factor Analysis

FTIR   Fourier Transform Infrared Spectroscopy

HHP   High Hydrostatic Pressure

LOX   Lipoxygenase

MIR   Mid Infrared

MS   Manosonication

MTS   Manothermosonication

NIR   Near Infrared

NMR   Nuclear Magnetic Resonance

NN   Neural Networks

PCS   Pig Citrate Synthase

PG   Polygalacturonase

PLS   Partial Least Squares

PME   Pectin Methylesterase

POD   Peroxidase

PPO   Polyphenol Oxidase

TS   Thermosonication

CHAPTER 1

INTRODUCTION

Enzymes are important in catalyzing chemical reactions in almost all biological processes. Due to its substrate specificity, enzymes can speed up reactions by lower activation energy and at the end of the reaction remain unchanged. In fruits and vegetables, enzymes play important role in detecting the quality attributes such as texture, flavor, color, nutritional value and sensorial properties (Tsou 1986, Oey 2010).

1.1. Enzymes and Their Structure

With the exception of a small group, all enzymes are proteins. Proteins are polymers of amino acids joined together by a peptide bond between the carboxylic acid group of one amino acid and the amino group of the next. There are 20 common amino acids in protein. Amino acids can be divided into four different classes depending on the structure of their side chains: nonpolar, polar uncharged, negatively charged and positively charged. The properties of the amino acid side chains determine the properties of the proteins they constitute (Platis et al. 2006).

Four levels of protein structure exist: primary, secondary, tertiary and quaternary. The primary structure of a protein refers to the linear sequence in which the constituent amino acids are covalently linked through amine bonds, also known as peptide bonds (Damodaran et al. 2007). The primary structure is responsible for the enzymatic activity.

Secondary structure is known as hydrogen bonded regions of the polypeptide chains of enzymes. Secondary structure of proteins consists of helices, plated sheets, β turns, and random coils involving the backbone of the polypeptide chains. In proteins, only three types of helical structures, namely α-, 3_{10}-, β-helix, are found. Among the three helical structures, the α-helix is the major form found in proteins and it is the most stable. The α-helix is stabilized by hydrogen bonding. In this structure, each backbone N-H group is hydrogen bonded to the C=O group of the fourth proceeding residue. The α-helix can be thought of as having a structure similar to a coil or spring. The "hole" running down the center of the α-helix is too narrow to permit water to enter, so the α-helix is stabilized against disruption by hydrogen-bonding agents such as water (Whitaker 1994, Platis et al. 2006. Damodaran et al. 2007).

The β-sheet is an extended structure with specific geometries. In this extended form, the C=O and N-H groups are oriented perpendicular to the direction of the chain, and therefore hydrogen bonding is possible only between segments, and not within a segment. The β-strands are usually about 5-15 amino acid residues long. In proteins, two β-strands of the same molecule interact via hydrogen bonds, forming a sheet – like structure known as β-pleated sheet. The β-sheet can be visiualized as a series of parallel strings laid on top of an accordion-folded piece of paper. Depending on the N → C directional orientations of the strands, two types of β-pleated sheet structures, namely parallel β- sheet and antiparallel β- sheet, can form. In parallel β-sheet the directions of the β-strands run parallel to each other, whereas in the other they run opposite to each other (Platis et al. 2006, Damodaran et al. 2007).

Proline is a special amino acid becuse of its unique structure. Proline involves imino structures. Introduction of proline into the sequence creates a permanent bend at that position. Therefore, the presence of proline in α-helix or β-sheet disrupts the secondary structure at that point. The presence of a glycine residue confers greater than normal flexibility on a polypeptide chain. This is due to the absence of a bulky side chain, which reduces steric hindrance (Whitaker 1994, Platis et al. 2006).

The β-turn is another frequently observed structural unit. This occurs when the main chain sharply changes direction using a bend composed of four successive residues, often including proline and glycine. In these units the C=O group of residue i is hydrogen bonded to the NH of residue i + 3 instead of i + 4 as in the α-helix (Platis et al. 2006).

Tertiary structure refers three-dimensional form of a protein. A number of different types of bonds are involved in maintaining the tertiary structure of proteins. These include electrostatic bonds, hydrogen bonds, hydrophobic bonds (van der Waals forces), dipolar bonds and disulfide bonds. The most stable bond is the disulfide bond. The disulfide bond is the covalent bond which can be formed between two cysteine side chains under oxidizing conditions. Hydrogen bonding results from the formation of hydrogen bridges between appropriate atoms; electrostatic bonds are due to the attraction of oppositely charged groups located on two amino acid chains. Van der Waals bonds are generated by the interaction between electron clouds (Whitaker 1994, Platis et al. 2006. Damodaran et al. 2007).

Quaternary structure contains more than one polypeptide chain (Damodaran et al. 2007). The four levels of enzyme structure are illustrated in Figure 1 (Nelson and Cox 2008).
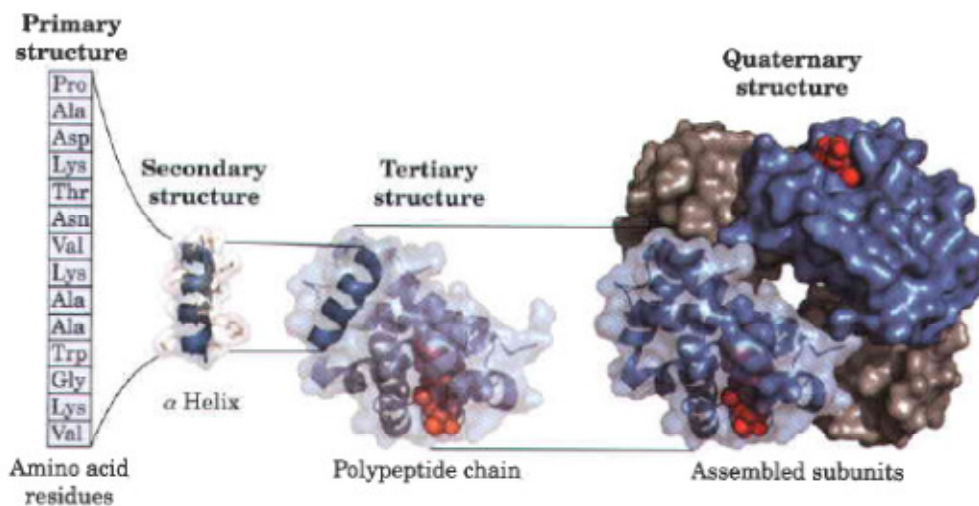
Figure 1. Protein structure, from primary to quaternary structure (Nelson and Cox 2008)

These three dimensional structures provide to bring together amino acid side chains that are distant from one another along the polypeptide chain. The active site is formed by amino acid groups from different parts of the linear polypeptide chain, brought into proximity in the folded enzyme structure.

Enzymes are responsible for numerous catalytic reactions, which are carried out on their active sites. Enzymes take part in the reaction, speed up reactions. If an enzyme is denatured, catalytic activity is usually lost. If an enzyme is broken down into its amino acids, its catalytic activity is always destroyed. Thus the primary, secondary, tertiary, and quaternary structures of enzymes are essential to their catalytic activity (Tsou 1986, Nelson and Cox 2008).

1.2. Food Enzymes and Related Quality Attributes

Enzymes, although minor constituents of many foods, play a major role in foods. Food enzymes can be generally classified in two ways: those that are added to foods to cause a desirable change and those that exists in foods and which may or may not be responsible for reactions that affect food quality (Damodaran et al. 2007).

Enzymes in fruit and vegetable products affect the texture, color, flavor and nutritional quality of the product. Some of these enzymes are polyphenol oxidase (PPO), which is responsible for browning and off color development, peroxidase, responsible for adverse changes in the flavor and color, lipoxygenase (LOX), which can contribute to off-flavor development, polygalacturonase (PG) and pectin methylesterase (PME), involved in the degradation of pectins and affect product viscosity or texture (Anthon and Barrett 2002, Versteeg et al. 1980).

1.2.1. Polyphenol oxidase

Enzymes related to color quality of foods are phenol oxidases, peroxidases, and other oxidoreductases. Polyphenol oxidases and peroxidases degradate phenolic compounds in the presence of oxygen and they form brown polymers called melanines (Tomas-Barberan and Espin 2001, Damodaran et al. 2007).

Phenol oxidases are the main cause of enzymatic browning that is associated with color quality loss during post-harvest storage, and processing, in damaged fruits and vegetables. In addition to color quality loss, enzymatic browning is also harmful to nutritional value of foods (Hendrickx et al. 1998, Ludikhuyze et al. 2003, Wu et al. 2008).

Polyphenol oxidase (PPO; monophenol, dihydroxy-L-phenylalanine: oxygen oxidoreductase, E.C 1.14.18.1) contains copper. Tyrosinase, cresolase, catecholase, diphenolase and phenolase are the different names of this enzyme. PPO is bound to

the membrane of chloroplasts whereas phenolic compounds are found in vacuoles in plant tissues. Thus, enzymes and substrates are seperated and this prevents enzymatic browning. After damaging this physiological barrier, phenolic compounds are oxidized rapidly (Tolbert 1973, Walker 1995, Tomas-Barberan and Espin 2001, Ludikhuyze et al. 2003).

The enzyme is generally found in all plants, but it is in particularly high concentration in potatos, peaches, apples, bananas, avocados, tea leaves, coffee beans, and tobacco leaves and also mushrooms (Whitaker 1994).

Phenol oxidases or tyrosinases oxidize phenolic compounds to quinones in the presence of oxygen. PPO catalyzes two different reactions: cresolase (monophenolase or hydroxylase) and catecholase (diphenolase or oxidase) activity. Cresolase activity involves the hydroxylation of monophenols composing *o*-diphenolic compounds. Unlike the cresolase activity, catecholase activity oxidizes two *o*-diphenol molecules to two *o*-quinones. PPO always displays catecholase activity (Mayer and Harel 1979, Mason 1956, Tomas-Barberan and Espin 2001, Wu et al. 2008). Figure 2 shows the cresolase and catecholase activities of PPO (Ludikhuyze et al. 2003).

The quinones are highly reactive substances. They react with other quinones, amino acids, or proteins to produce brown compounds. These compounds deteriorate food quality and affect nutritional and organoleptic properties of foods (Vamos-Vigyazo 1981).
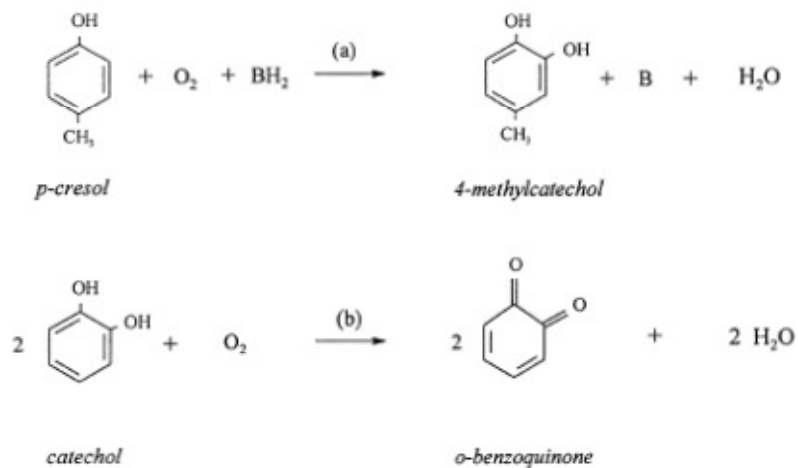
Figure 2. Cresolase (a) and catecholase (b) activities of PPO (Ludikhuyze et al. 2003).

1.3. Effect of Heat on Enzyme Inactivation

Fruit and vegetable products are exposed to some treatments in order to inactivate microorganisms and quality related food enzymes that cause a problem during processing and storage. Thermal treatment, such as blanching, pasteurization or sterilization, is the most commonly used method for industrial inactivation of these enzymes.

Although blanching is a mild heat treatment, it is not used a method of preservation by itself. Most of the vegetables and some of the fruits are blanched before further processing, such as canning, freezing or dehydration. The product is heated to a predetermined temperature, hold for a time and then cooled rapidly during blanching. There are three ways of blanching produce: water, steam or microwave blanching. Commercial blanching is carried out at temperatures close to 100° C for two to five minutes in either a water bath or a steam chamber. A large number of naturally occurring enzymes are denatured at relatively low temperatures, and it is likely that a blanching operation would be used to achieve this (Grandison 2006).

Pasteurization is a heat treatment, in which food is heated to below $100^{o}C$, used to extend the shelf life of food at low temperatures. Pasteurization causes minimal changes in food when inactivates enzymes and microorganisms, relatively heat sensitive. In sterilization, food products are heated at temperatures above $100^{o}C$ ($110-125^{o}C$) and for a long time to destroy microbial and enzyme activity. Sterilization causes the complete destruction of all viable organisms in food products and allows storing the products at ambient temperatures, with extended shelf life. Practically, complete sterilization leads to deterioration in food products. For this reason, commercial sterilization is used in practice. Commercial sterilization is defined as "a product that has been optimally processed so that under normal conditions, the product will never spoil nor endanger the health of consumer and also retain the organoleptic properties and nutrients" (Fellows 2000, Ramesh 2007).

Some food industries, such as production of citric juices, tomato pastes and juices are concerned with the inactivation of deleterious enzymes (Sala et al. 1995). In milk some of the enzyme, lipase and phosphatase are destroyed by pasteurization, peroxidase and xanthine oxidase are inactivated by sterilization (Underkofler 1980). Inactivation of polyphenol oxidase and peroxidase that are responsible for browning and inactivation of pectic enzymes that is responsible for cloud stability is important for fruit juices (Lewis and Heppel 2000).

Many studies on enzyme inactivation during heat processing have been carried out by several researchers. Güneş and Bayındırlı (1993) studied POD and LOX inactivation and ascorbic acid retention during water and microwave blanching of peas, green beans and carrots. LOX and POD were used as blanching indicator enzymes during the experiments. When LOX was selected as the indicator enzymes ascorbic acid retention during blanching was higher in vegetables. Also ascorbic acid retention was found to be higher in microwave compared to water blanched vegetables.

McCord and Kilara (1983) studied the control of polyphenol oxidase (E.C. 1.14.18) activity by the use of citric acid. It was reported that the enzyme was inactivated at pH 4.0 and was stable to 10 min exposures at 25 °C in the pH range 4.0-8.0. At pH 6.5 the enzyme was detected as active at 45 °C but no activity detected at 70 °C and thermal inactivation followed pseudo first-order kinetics.

Peroxidase (POD) inactivation was studied during blanching at different constant temperatures in peaches, carrots and potatoes by Tijskens et al. (1997). Bound and soluble POD were used in this study. Both of the enzymes are susceptible to heat denaturation.

Yemenicioğlu et al. (1997) were determined the heat inactivation parameters of PPO from different apple cultivars at three different temperatures (68, 73 and 78°C). PPO followed a first order kinetic model and its activity of the enzyme initially increased and then decreased. Heat stability of PPO in apple was compared to PPO in other fruits. Results indicated that PPO in apples was generally more heat-stable than PPO in most fruits.

Anthon and Barrett (2002) studied kinetic parameters of PPO, POD and LOX in carrots and potatoes during thermal inactivation. Samples were heated between 60 and 85 °C for different times. POD activity decreased by 50% in both carrots and potatoes at the temperatures studied. Peroxidase activity followed first-order inactivation kinetics in both vegetables. LOX and PPO were investigated in potatoes but not investigated in carrots because LOX and PPO is found only in the peel of carrots, which is generally discarded during commercial processing. Inactivation of PPO and LOX did not follow first-order kinetics.

Kinetic parameters of pectin methylesterase (PME), polygalacturonase (PG), and peroxidase (POD) in tomato juice were determined by Anthon et al. (2002). The inactivation kinetics for all three enzymes was determined in both hot-break processing (95°C) tomatoes and cold-break processing (60°C) tomatoes. Inactivation

of POD in tomato juice followed simple first-order kinetics during thermal treatment. Experimental results indicate that POD in tomatoes is not stable during heat treatment.

Thermal inactivation kinetics of peroxidase (POD) and lipoxygenase (LOX) from broccoli (florets), green asparagus (tip and stem), and carrots (cortex and core) extracts were determined in the temperature range of 70 to 95°C for 0 to 600 s (Morales-Blancas et al. 2002). Experimental results indicate that the kinetics of both enzymes followed a biphasic first-order model. However, LOX in asparagus showed a monophasic first-order behavior at 70°C. In carrots, LOX activity was not detected.

In another study, effect of different water blanching conditions on the quality of pea during frozen storage was studied. POD and LOX were used as blanching indicator enzymes. It was found that POD was more heat stable than LOX in peas and no regeneration of LOX and POD activities was determined during storage at – 18°C. In this study, it was found that 90% reduction in POD activity was achieved during a blanching time of 2.0 min at 80°C (Gökmen et al. 2005).

Inactivation of POD, PPO, and LOX in paprika and chili during thermal treatment were studied by Schweiggert et al. (2005). It could be shown that the lowest stability was observed for PPO and this enzyme was completely inactivated by heating at 80°C for 10 min in both paprika and chili. LOX was inactivated largely at 90°C for 5 min and at 100°C for 5 min. 98% reduction was observed in POD activities in chili and paprika powder.

Thermal inactivation kinetics of tomato LOX was studied by Anese and Sovrano (2006). Tomatoes were inactivated in the temperature range of 80-98°C for 0 - 150 min. Their results showed that tomato lipoxygenase had a high thermal resistance. They suggested that applied blanching treatments may not be adequate to achieve complete inactivation.

Mustapha and Ghalem (2007) studied the effect of thermal treatment (55°C/20 min) on polyphenol oxidase (PPO) and peroxidase (POD) in Algerian dates. 20 min thermal treatment was not sufficient to inactivate the enzymes. Activities of POD and PPO during heat treatment decreased.

Effect of steam blanching on polyphenoloxidase, peroxidase in mango (Mangifera indica L.) was studied by Ndiaye et al. (2009). Effect of different steam blanching time on PPO and POD activity, and the color of processed mango were determined. POD was completely inactivated at 5 min and PPO was completely inactivated at 7 min steam blanching. Color loss becomes more important when blanching time exceeds 5 min.

Gouzi et al. (2012) studied the inactivation of polyphenol oxidase (PPO) from mushroom *Agaricus bisporus* during thermal treatment. Thermal inactivation of the enzyme was determined between 50 and 73 °C and significant inactivation was observed when the temperature increased.

1.4. Effect of Ultrasound on Enzyme Inactivation

Generally, thermal treatments are applied to many of the foods to inactivate microorganisms and enzymes. However, heat destroys nutritional components of foods and affects physical characteristics such as texture, color, and flavor. In recent years consumer demand for convenient, fresh-like, safe, high quality food products has grown. These demands have encouraged the researchers to use minimal thermal methods. Non-thermal technologies such as ultrasound, high hydrostatic pressure, super critical carbon dioxide, pulsed electric fields represent a more promising alternative to traditional thermal processing. Therefore, the sensory characteristics and nutritional value of foods are maintained higher quality products are obtained (Fellows 2000).

One "new" or emerging technology receiving a great deal of attention is ultrasound. Ultrasound has attracted a great deal of interest because of the effect on physical, biochemical, and microbial properties of foods. Systematic studies of physical, chemical and biological effects produced by ultrasound began in early 1900s. The late 1920s was an important time in ultrasound research with potential application in the food industry, with a number of important ultrasound effects identified. During this time, various researchers reported that ultrasound could be used to rupture microorganisms; inactivate enzymes; emulsify oil and water; atomize liquids; cause agitation inside individual plant; accelerate chemical reactions; and degas liquids (Torley and Bhandari 2007).

There are different types of ultrasonic apparatus commercially available for small- or large-scale ultrasound applications including whistle reactors, ultrasonic baths, and probe systems. A whistle reactor uses a mechanical ultrasonic source that relies on a stream of liquid flowing past a metal blade to cause vibration. "With ultrasonic baths, the transducer is bonded to the base or sides of the tank and the ultrasonic energy is delivered directly to the liquid in the tank. However, with probes, the high power acoustic vibration is amplified and conducted into the media by the use of a shaped metal horn; and the shape of the horn will determine the amount of signal amplification" (Leadley and Williams 2006, Torley and Bhandari 2007).

Ultrasound waves, similar to sound waves, have a frequency that is above 20 kHz and cannot be detected by the human ear. Transmission of sound occurs due to ordered and periodical movements of the media, with motional energy passed on to adjacent molecules without transfer of matter. Ranges of the sound can be divided into;

(1) Low-power, high-frequency ultrasound (<1 W/cm^2; >100 kHz) is normally used as a non-destructive analytical method to determine the composition, structure or flow rate of foods.

(2) High-power, low- frequency ultrasound (10-1000 W/cm^2; 20-100 kHz) is used at higher frequencies to cause physical disruption of tissues, create emulsions, clean equipment, or promote chemical reactions (e.g. oxidation) (Fellows 2000, Torley and Bhandari 2007).

Combining ultrasound with pressure, temperature, or pressure and temperature treatments increases its effect in enzyme and microbial inactivation. Combinations of ultrasound with heat (thermosonication), pressure (manosonication) and pressure & heat (manothermosonication) are used. In thermosonication method (TS), the product is subjected to ultrasound and mild heat at the same time. It is considered to decrease temperatures and times in processing of pasteurization or sterilization that achieve the same lethality values as with conventional processes. Manosonication (MS) combines ultrasound with pressure (100 - 300 kPa) at low temperature in order to provide inactivation of enzymes and/or microorganisms. In manothermosonication (MTS) combination of ultrasound with moderate temperature and moderate pressure are generally used in order to achieve higher microbial and enzyme inactivation. Therefore, shorter times or lower temperatures are used in order to achieve the same inactivation (Demirdöven and Baysal 2009).

Lopez and Burgos (1995) inactivated lipoxygenase by using MTS. They determined the sonication effect of enzyme concentration, KCl, physical parameters, pH, sugars and glycerol on LOX in order to determine inactivation efficiency of MTS. MTS efficiency for the inactivation of LOX, in phosphate buffer (pH 6.5) increased with ultrasound amplitude in the range of 0-104 μm at treatment temperatures (67.5-76.3°C). In MTS when ultrasound amplitude increased, activation energy *(E$_a$)* decreased and it was found to be lower than in thermal enzyme inactivation. It was reported that effect of the pH of the medium on the temperature dependence of the inactivation rate was observed. *E$_a$* increased with increasing pH for both MTS and heat treatment but pH dependence was found to be more in MTS than in heat inactivation. LOX followed first order kinetic model for MTS inactivation. LOX

concentration did not affect thermal stability. However, LOX concentration increased MTS resistance increased linearly.

In another study inactivation of lipoxygenase in soy flour suspension (1%) was determined. The suspension was subjected to sonification for different time, and frequencies. The time of exposure, pH, and the amplitude of ultrasound influenced the inactivation of the enzyme. Inactivation was not achieved after 3 h ultrasound treatment at pH > 5.0. However, at pH ≤ 5.0, the activity decreased when the time increased and approximately 70-85% of inactivation was observed at pH 5.0 and 4.0 respectively under similar conditions. It was also determined the effect frequency on the inactivation of enzyme. Enzyme was not affected exposure to cavitating 30 kHz ultrasound for 60 min at any of the pH studied. However, enzyme activity decreased at frequency >30 kHz and at a pH of 5.0 or below. The results showed that the enzyme was irreversibly inactivated by ultrasound and no reactivation was observed after 24 h storage (Thakur and Nelson 1997).

De Gennaro et al. (1999) studied the inactivation of horseradish peroxidase by TS. The inactivation was performed at 80°C for different ultrasonic frequencies (20, 40, and 60 kHz), for different times and for different ultrasonic powers (0 to 120 W). Continuous and batch mode were used. In all conditions the inactivation of the enzyme followed first order kinetics. It was reported that the decimal reduction time of peroxidase at 80°C, decreased from 65 to 10 min during ultrasound treatment.

The inactivation kinetics of peroxidase in watercress (Nasturtium officinale) was studied by Cruz et al. (2006). Peroxidase was inactivated by using heat and the combined heat/ultrasound (TS) treatment in the temperature range of 40-92.5^{o}C. The enzyme kinetics showed a first-order biphasic inactivation model in the heat blanching processes. The enzyme kinetics showed a first-order model in the TS treatments. The activation energy, the rate of reaction at a reference temperature and the initial relative specific activity were, respectively, E_{a3} = 496 ± 65 kJmol^{-1}, $k_{387.5^{o}C}$ = 10 ± 2min^{-1}, proving that the enzyme became more heat labile. Higher enzyme

inactivation was obtained for TS for same time and temperatures above 85°C compared to the thermal treatment. It was concluded that TS treatments improve the quality of the product.

1.4.1. Effect of Ultrasound on Mushroom PPO

Although, there have been too many studies about POD, LOX, and PPO inactivation during ultrasound treatment, there is very little information about mushroom PPO after ultrasound inactivation in literature.

POD, mushroom PPO, and LOX were inactivated by using MTS (Lopez et al. 1994). The results showed that the combination of heat and ultrasound had synergistic effects on the enzymes and heat treatment must require for inactivation. Combined treatment did not alter the z value of peroxidase, estimated to be 26°C, but changed that of lipoxygenase. It was found that when the amplitude increased, efficiency increased. While amplitudes increased, decimal reduction times at constant temperature decreased in all cases. It was revealed that increasing pressure caused increase in the inactivation rate.

Cheng et al. (2013) studied the effect of thermosonic and thermal treatments on the inactivation kinetics of polyphenol oxidase (PPO) in mushroom (*Agaricus bisporus*) in 55-75°C temperature range. They found that the inactivation kinetics of PPO showed a first-order kinetics (R^2 = 0.941-0.989) in both processes. It was reported that the D values during thermal inactivation varied from 112 ± 8.4 min to 1.2 ± 0.07 min while they varied from 57.8 ± 6.1 min to 0.88 ± 0.05 min during thermosonic inactivation and the D values of PPO decreased by 1.3-3 times during thermosonic inactivation compared to the D values of PPO during thermal inactivation at the same temperature range. They concluded that ultrasound and heat combination was found to synergistically increase the inactivation of PPO.

1.5. Enzyme Inactivation Mechanism by Ultrasound

"The main mechanisms by which enzyme inactivation is thought to occur are cavitation, localized heating and free radical formation. Cavitaion takes place when ultrasound passes through a liquid medium, causing alternate rarefactions (negative pressure) and compressions (positive pressure). If the ultrasound waves are of sufficiently high amplitude, bubbles are produced. These bubbles collapse with differing intensities and it is thought to be a major contribution to cellular disruption. The mechanisms involved in cellular disruption may include shear forces generated during movement (subcellular turbulance) of the bubbles or sudden localised temperature (5000 K) and pressure (50 MPa) changes caused by bubble collapse (Leadley and Williams 2006, Demirdöven and Baysal 2009 and Manas et al. 2006). Sonication also promotes chemical reactions involving $H^{+ \cdot}$ and OH^{-} free radicals, formed by the decomposition of water inside the oscillating bubbles. Free radicals so produced could be scavenged by some amino acid residues of the enzymes participating in structure stability, substrate binding, or catalytic functions (Lopez et al., 1994). Under these extreme conditions, sonication could cause the breakdown of hydrogen bonding and van der Waals interactions in the polypeptide chains, leading to the modification of the secondary and tertiary structure of the protein. With such changes in the protein secondary and tertiary structure, the biological activity of the enzyme is usually lost" (Mawson et al. 2010).

The inactivation of enzymes is generally represented with simple kinetic approaches in the literature. The investigation of inactivation mechanism of the fruit and vegetable enzymes by using nonthermal treatments takes an interest in the research area.

1.6. Infrared Spectroscopy

"Infrared spectroscopy is a vibrational spectroscopic technique. The chemical bonds in the molecules have specific frequencies at which they vibrate, corresponding to energy levels. These vibrational frequencies are determined by the mass of the atoms, the shape (geometry) of the molecule, and the stiffness of the bonds and the periods of the associated vibrational coupling. A specific vibrational mode has to be associated with changes in the permanent dipole in order to be active in the infrared area. Diatomic molecules have only one bond, which may stretch (i.e. the distance between two atoms increases or decreases). More complex molecules may have many bonds, and vibrations can be conjugated leading to two possible modes of vibration: stretching and bending (i.e. the position of the atom changes relative to the original bond axis). In such cases the vibrations lead to infrared absorptions at characteristic frequencies that may be related to chemical groups" (Karoui et al. 2008).

"Three types of vibrational spectroscopy are generally distinguished: near-infrared (NIR), mid-infrared (MIR), and Raman spectroscopy. The NIR region lies between 12 500 and 4000 cm^{-1} (0.8-2.5 µm), and NIR spectroscopy operates with a light source from which the sample absorbs specific frequencies corresponding to overtones and combination bands of vibrational transitions of the molecule primarily of OH, CH, NH and CO groups. The MIR region of the electromagnetic spectrum lies between 4000 and 400 cm^{-1} (2.5-50 mm) and is associated mainly with fundamental molecular stretching and bending vibrational frequency – i.e. the frequencies of the fundamental vibration modes of the molecules (from the stable vibrational state to the first excited vibrational state in the electronic ground state)" (Karoui et al. 2008).

"The mid-infrared spectrum (4000 – 400 cm^{-1}) can be approximately divided into four regions and the nature of a group frequency may generally be determined by the region in which it is located. The regions are generalized as follows: the X–H

stretching region (4000 – 2500 cm^{-1}), the triple-bond region (2500 – 2000 cm^{-1}), the double-bond region (2000 – 1500 cm^{-1}) and the fingerprint region (1500 – 600 cm^{-1}). The fundamental vibrations in the 4000 – 2500 cm^{-1} region are generally due to O–H, C–H and N–H stretching. O–H stretching produces a broad band that occurs in the range 3700 – 3600 cm^{-1}. By comparison, N–H stretching is usually observed between 3400 and 3300 cm^{-1}. This absorption is generally much sharper than O–H stretching and may, therefore, be differentiated. C–H stretching bands from aliphatic compounds occur in the range 3000 – 2850 cm^{-1}. If the C–H bond is adjacent to a double bond or aromatic ring, the C–H stretching wave number increases and absorbs between 3100 and 3000 cm^{-1}".

"Triple-bond stretching absorptions fall in the 2500 – 2000 cm^{-1} regions because of the high force constants of the bonds. C≡C bonds absorb between 2300 and 2050 cm^{-1}, while the nitrile group (C≡N) occurs between 2300 and 2200 cm^{-1}. These groups may be distinguished since C≡C stretching is normally very weak, while C≡N stretching is of medium intensity. These are the most common absorptions in this region, but you may come across some X–H stretching absorptions, where X is a more massive atom such as phosphorus or silicon. These absorptions usually occur near 2400 and 2200 cm^{-1}, respectively".

"The bands in the 2000 – 1500 cm^{-1} region are due to C=C and C=O stretching. Carbonyl stretching is one of the easiest absorptions to recognize in an infrared spectrum. It is usually the most intense band in the spectrum and depending on the type of C=O bond, occurs in the 1830 – 1650 cm^{-1} region. Note also that metal carbonyls may absorb above 2000 cm^{-1}. C=C stretching is much weaker and occurs at around 1650 cm^{-1}, but this band is often absent for symmetry or dipole moment reasons. C=N stretching also occurs in this region and is usually stronger" (Stuart 2004).

"Raman also lies in a region similar to MIR; in contrast with the other two techniques, it involves a scattering process that arises when the incident light excites

18

molecules in the sample, which subsequently scatter the light. Most of this scattered light is at the same wavelength as the incident light, but some is scattered at a different wavelength. The process leading to this "inelastic" scatter is called the Raman Effect" (Karoui et al. 2008).

"In practice, to measure a sample, a beam of infrared light passes through the sample and the absorbed energy at each wavelength is recorded. This can be done in two different ways; by scanning through the spectrum with a monochromatic beam, which changes in wavelength over time, or by using a Fourier transform system to measure all the wavelengths at the same time. As a result, taking into account the effects of all the different functional groups, an absorbance (or transmittance) spectrum is obtained showing at which wavelengths the sample absorbs the infrared light, thus allowing interpretation of the chemical bonds" (Karoui et al. 2008).

Infrared spectroscopy has proved to be a powerful tool for the study of biological molecules. This has been applied for long time for the characterization of proteins and lipids (Stuart 2004).

1.6.1. Fourier Transform Infrared Spectroscopy

There are lots of analytical tools to study protein conformation, such as X-Ray crystallography, Fourier transform infrared spectrometry (FTIR), nuclear magnetic resonance (NMR) spectroscopy, circular dichroism spectroscopy (CD) (Shi et al. 2003 and Haris and Severcan 1999).

Circular dichroism spectroscopy is good for characterizing protein structure, compares the structures of a protein obtained from different sources, and studies the conformational stability of a protein under stress (Greenfield 2006). X-ray crystallography and NMR are used to achieve the complete structure determination of a protein at high resolution but they have some disadvantages. The process of X-ray crystallography is very slow and requires high quality single crystals, which are

not always available, and the structure of a protein in a crystal may not always relate to its structure in solution. NMR spectroscopy can be used to determine the structure of a protein in solution but the technique is presently limited to small proteins (30 kDa) (Haris and Severcan 1999).

FTIR has recently become very popular for structural characterization of proteins. It provides high-quality spectra with very small amount of protein (10 μg) and also the size of the protein is not important. It has a large application range from small soluble proteins to large membrane proteins. It has also short measuring time with relatively low costs compared to the cost of X-ray diffraction, NMR and CD spectroscopic equipments (Haris and Severcan 1999, Carbonaro and Nucara 2010, Severcan et al. 2001, Barth 2007).

"Fourier-transform infrared (FTIR) spectroscopy is based on the idea of the interference of radiation between two beams to yield an interferogram. The latter is a signal produced as a function of the change of pathlength between the two beams. The two domains of distance and frequency are interconvertible by the mathematical method of Fourier-transformation. The basic components of an FTIR spectrometer are shown schematically in Figure 3 (Stuart 2004). The radiation emerging from the source is passed through an interferometer to the sample before reaching a detector. Upon amplification of the signal, in which high-frequency contributions have been eliminated by a filter, the data are converted to digital form by an analog-to-digital converter and transferred to the computer for Fourier-transformation".

| Source | Interferometer | Sample | Detector | Amplifier | Analog-to-digital converter | Computer |

Figure 3. Basic components of an FTIR spectrometer (Stuart 2004).

"The most common interferometer used in FTIR spectrometry is a Michelson interferometer, which consists of two perpendicularly plane mirrors, one of which can travel in a direction perpendicular to the plane (Figure 4) (Stuart 2004). Between

the mirrors there is a beam-splitter, normally made up of KBr coated with germanium (for the MIR region). The beam-splitter splits a beam of light that enters (incident beam) into two new beams, one reflected onto the moving mirror and the other onto the fixed (stationary) mirror. The two beams are then reflected back and recombined at the beam-splitter. Owing to path differences between the mirrors, both beams undergo constructive and destructive interferences. The recombined beam is then passed on towards the sampling area, where it interacts with the sample. The transmitted, diffused or reflected light reaches the detector, where the energy is digitized, resulting in an output signal consisting of the sum of cosine waves. This is the interferogram. This interferogram consists of the intensity of energy measured versus the position of the moving mirror (function of time domain), and contains basic information about frequencies and intensities, but is not directly interpretable. The interferogram is then converted into a conventional infrared spectrum (function of frequency domain) by the mathematical function known as the Fourier transforms" (Karoui et al. 2008).
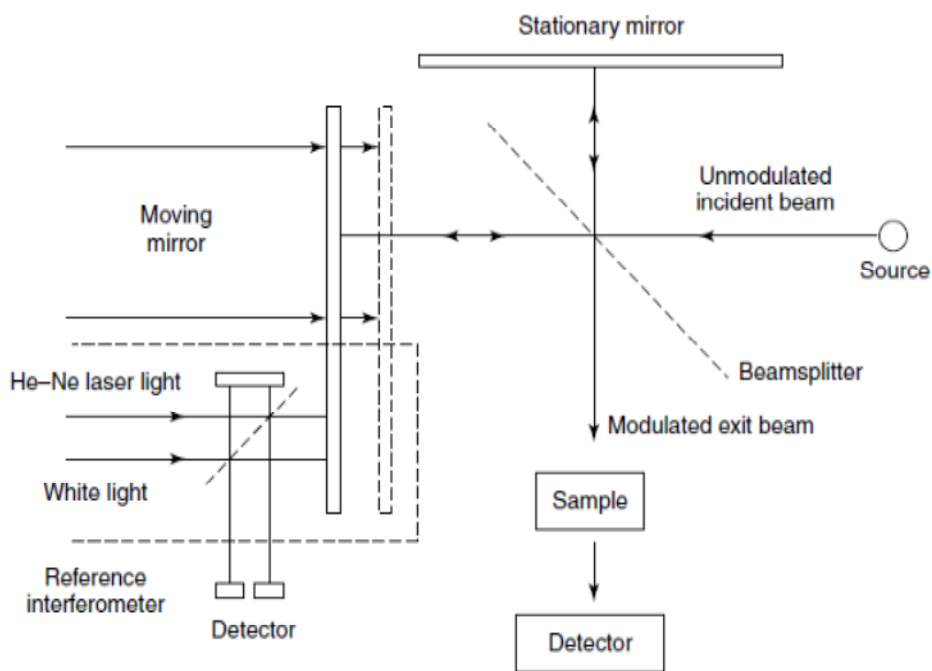
Figure 4. Schematic of a Michelson interferometer (Stuart 2004).

The vibrational spectra of proteins provide information about protein secondary structure from an analysis of the amide bands (Mantsch 2001). These are called amide A, amide B and amides I-VII. The amide I and amide II bands are more useful for conformational studies than others.

The amide I band is the most useful infrared band for the analysis of the secondary structure of proteins. It occurs between 1700 and 1600 cm^{-1}. The amide I band represents 80% of the C=O stretching vibration of the amide group, coupled to the in plane N–H bending and C–N stretching modes. The exact frequency of this vibration depends on the nature of the hydrogen bonding involving to C=O and N–H groups and this is determined by the particular secondary structure adopted by the protein. Proteins generally possess a variety of domains containing polypeptide fragments in different conformations. The amide I band consists of helices, β-structures, turns and random structures.

The amide II bands represents mainly N–H bending (60%), with some C–N stretching (40%). As with the amide I band, it is possible to split to amide II band into components which depend on the secondary structure of protein. The amide II band is observed at 1550 cm^{-1} (Stuart and Ando 1997, Stuart 2004).

It can be estimated the percentage of each structure element like α-helix, β-structure and random coil structure by analyzing the amide I and/or amide II band regions. Table 1 shows relationships between secondary structures of proteins and the frequencies of amides I and II. However, detailed quantitative analysis of amide I and amide II bands is not always an easy task because a number of bands due to various secondary structures overlap heavily. For the analysis of the overlapping amide bands, various spectral analysis methods have been proposed. Most are frequency-based methods which rely on peak assignments in either second derivative or deconvoluted spectra.

Table 1 Secondary structures of protein and frequencies of amide I, and II bands (Stuart 2004).

Secondary structures	Infrared	
	Amide I	Amide II
α-helix	1655~1650	~1540
β-sheet -structure	~1690, 1680~1675, ~1640, ~1630	~1550
Random coil	1655~1645	1535~1530
β-turn	~1680, ~1660, ~1640	

The second derivative and deconvolution enhance band resolution, enable one to identify the different structures in a protein and also to monitor structural variations induced by protein denaturation. Figure 5 illustrates the original, deconvoluted and derivative spectra of an amide I band (Stuart and Ando 1997).
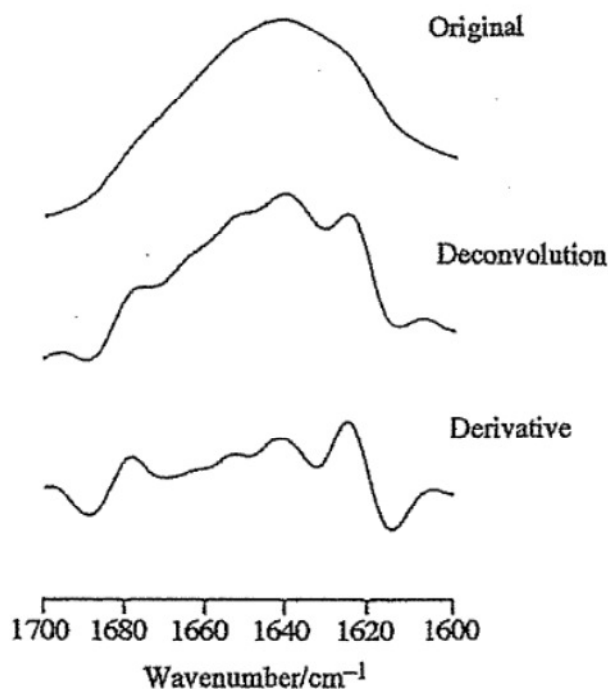
Figure 5. The original, deconvoluted and derivative spectra of an amide I band (Stuart and Ando 1997).

To determine the quantitative amounts of different protein secondary structures (α-helixes, β-sheets, etc.,) curve-fitting, partial least squares analysis, factor analysis, and neural networks (NN) are used. For quantitative analysis curve-fitting is often employed. Figure 6 shows a curve-fitting process (Severcan et al. 2001, Stuart 2004, Carbonaro and Nucara 2010). Partial least squares (PLS) methods involve matrix operations and factor analysis (FA) methods use functions to model the variance in a data set (Stuart 2004). Neural networks (NN) are reported to be effective way to predict the secondary structure of proteins from FTIR spectra (Severcan et al. 2001).
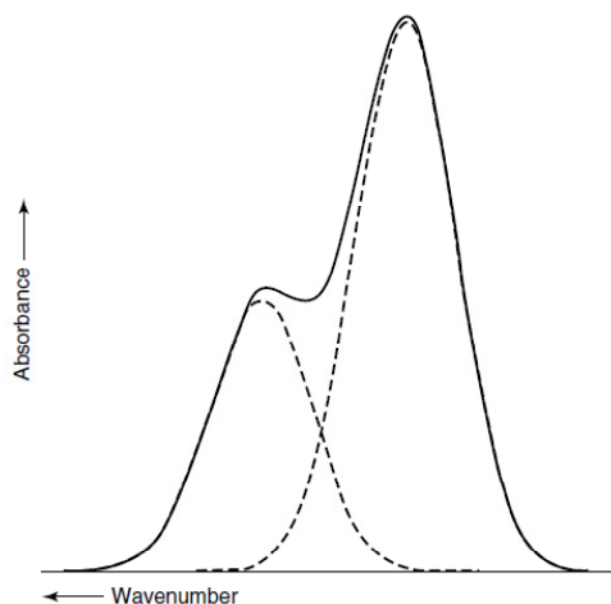
Figure 6. Illustration of curve-fitting of overlapping infrared bands (Stuart 2004).

There have been lots of studies about protein conformation determined by FTIR spectroscopy during thermal, ultrasound and pressure treatment. Unfolding of pig citrate synthase (PCS) during thermal treatment was investigated by determining the changes in amide I band sub bands. The results indicated that irreversible change was observed in the inactivation (Severcan and Haris 2003). Secondary structure and conformation change of bovine serum albumin during heat treatment (Murayama and Tomida 2004), structural and functional changes of bovine serum albumin during

ultrasound treatment (Gülseren et al. 2007), and effect of pressure on structural behavior of bovine serum albumin (Savadkoohi et al. 2014) was investigated in the literature. However, little information was found about inactivation mechanism of food enzymes determined by using FTIR spectroscopy.

FTIR spectroscopic analysis of mushroom PPO was investigated in the temperature range 25 – 45 ℃. It was reported that tyrosinase was predominately α- helix, it was indicated by the presence of a strong band at 1651 cm^{-1}. The deconvoluted spectra of tyrosinase at different temperatures indicated that above 40 ℃ the secondary structure of the enzyme began to change with increasing temperature. A new band at 1616 cm^{-1} (aggregation band) appeared at 45 ℃ and its intensity increased with time (Tse et al. 1997). Weemaes et al. (1997) determined the change in the mushroom PPO enzyme after thermal and pressure treatment by using FTIR spectroscopy. Thermal treatment was applied to the enzyme up to 90°C. It was revealed that mushroom PPO was a heat sensitive enzyme and inactivated after temperatures 50°C. Furthermore, FTIR study showed that thermal denaturation of the enzyme was irreversible and change in the activity was due to the global conformational change of the enzyme. However, the enzyme was very pressure stable and FTIR-spectroscopy showed that changes in the structure of the enzyme due to the pressure and thermal treatment were different.

Smeller et al. (2003) studied the pressure stability of horseradish peroxidase (HRP). The conformational changes in the secondary structure of horseradish peroxidase were investigated by using FTIR spectroscopy during pressurization. It was reported that HRP was stable under high pressure with an unfolding midpoint of 12.0 ± 0.1 kbar.

Dirix et al. (2005) studied the stability of recombinant *Aspergillus aculeatus* PME (pectin methylesterase), an enzyme with high *β*-helix content, as a function of pressure and temperature. The conformational stability was monitored using FTIR (Fourier transform IR) spectroscopy. They observed protein unfolding followed by

amorphous aggregation, which makes the process irreversible, at temperatures above 50°C. It was reported that hydrostatic pressure greater than 1 GPa was necessary to induce changes in the enzyme's secondary structure. PME stability towards thermal denaturation was increased by pressure. Temperatures above 60°C were necessary to cause significant PME unfolding and loss of activity at 200 MPa.

Marchioni et al. (2009) investigated effect of ultrasound on proteins in aqueous solution with FTIR spectroscopy, UV–VIS spectroscopy, circular dichroism and light scattering. Secondary structures of six different proteins (myoglobin, cytochrome, lysozyme, trypsinogen, bovine serum albumin and α-chymotrypsinogen A) were determined. The experiment was performed using an ultrasound, which has frequency of 1 MHz, and sonication times of 10, 20, 30, 40, 50, and 60 min were used. It was found that a different behavior of proteins under sonication depends on the dominant secondary structure type (α-helix or β-sheets). The results suggested that the free radicals, produced by water sonolysis, affect significantly the changes of structural order.

The effect of ultrasound on the secondary structure of bovine serum albumin (BSA) was studied by FTIR (Liu et al. 2010). The relative contents of α-helix, beta-fold, beta-turn and random coil under different ultrasound treatment power and time were quantitatively determined via analysis of the amide I changes of infrared spectra of BSA using curve fitting method. It was reported that the secondary structure of BSA had variation trend from α-helix to beta-sheet, however, the relative contents random coil had not significant change.

The secondary structure of the mushroom PPO treated by the high hydrostatic pressure (HHP) was analyzed by Fourier transform infrared spectroscopy (FTIR). The α-helix content of mushroom PPO was decreased after HHP treatment, which indicated that the secondary structure of PPO changed (Yi et al. 2012).

The effect of ultrasound on the activity and conformation of α-amylase, papain and pepsin was investigated. It was reported that secondary structural components,

especially β-sheet, of these three enzymes were significantly influenced by ultrasound (Yu et al. 2014).

1.7. Aim of the Study

In food industry, enzymes play important role. Inactivation of some enzymes is crucial for many processes to have the desired food quality. Non-thermal preservation technologies or the combination of these technologies with heat treatment at low temperatures have gained importance for the inactivation of microorganisms and enzymes for the productions of foods with higher quality if compared with that of thermal processing of foods at high temperatures. The inactivation of enzymes is generally represented with simple kinetic approaches in the literature. The aim of this study is the investigation of changes in structure and activity of the mushroom polyphenol oxidase at different operation parameters such as non-thermal process main variable, temperature and time. Thermal and thermosonication (TS) treatments used in this study in order to inactivate PPO enzyme. After thermal and TS treatment changes in activity was determined. In order to understand the conformational changes of PPO after thermal and TS inactivation, secondary structure was analyzed by using FTIR spectroscopy. Detailed secondary structural analysis of mushroom PPO was done by neural network (NN) and curve-fitting analysis, using the amide I band (1700-1600 cm^{-1}) of FTIR spectra. Secondary structural changes compared with the change in the enzyme activity.

CHAPTER 2

MATERIALS AND METHODS

2.1. Enzyme Preparation and Activity Assay

Mushroom PPO (E.C 1.14.18.1) was purchased from Sigma (St. Louis, MO, USA). Lyophilized PPO was dissolved in 0.05 M phosphate buffer (pH 6.5). In activity determination experiments the enzyme was dissolved in phosphate buffer (pH 6.5, 0.05 M) at 0.08 mg/ml and for the conformational change experiments the enzyme was dissolved in phosphate buffer (pH 6.5, 0.05 M) at 70 mg/ml.

PPO activity was determined by measuring the rate of increase in absorbance at 420 nm. 2 ml of 50 mM potassium phosphate buffer (pH 6.5) and 0.3 ml of 0.2 M catechol solution in the phosphate buffer were mixed with 0.3 ml of the enzyme solution. The change in absorbance was followed by using BOECO (Model S22, Germany) UV-VIS spectrophotometer at room temperature ($25 \pm 1^{o}C$). Absorbance values were recorded at every 5 s for 3 min. Enzyme activity was calculated from the slope of the initial linear portion of the curve plotted with A_{420} versus time. One unit of PPO activity was defined as an increase in absorbance of 0.001/min at 420 nm. Enzyme activities were measured 3 times and expressed as residual activity (Weemaes et al. 1997; Sun and Song 2003).

2.2. Thermal Treatment at Ambient Pressure

Thermal treatment of mushroom PPO was performed at varying temperatures in the range of 20-80°C with a 10°C increment for 0, 5, 10, 15, 20, 25 and 30 min. The enzyme solutions (5 ml) in a glass tube with an inner diameter 16 mm and a depth of

50 mm were heated in temperature controlled dry block heater (HBR-48, Daihan Scientific Co. Ltd., Seoul, Korea) at selected temperatures and times. They were immediately transferred to ice water to stop thermal inactivation instantaneously and the enzyme activity measurement was performed after 10 to 60 min storage. All the experiments and measurements were performed triplicate (Weemaes et al. 1997).

2.3. Thermosonication (TS) Treatment

The ultrasonic processor (UP400S, Dr. Hielscher GmbH, Germany) with titanium alloy sonotrode was used for the application of high-power ultrasonic vibration. The ultrasonic transducer is integrated in a housing that is assembled with stand. The sonotrode is coupled to the ultrasonic processor via the horn.

The processor has an effective output power of 400 W in liquid media. "The ultrasonic processor generates longitudinal mechanical vibrations by means of electric excitation (reversed piezoelectric effect) with a frequency of 24 kHz. The power output of the processor can be steplessly adjusted between 20% and 100% of the maximum output. The set value remains constant under all operating conditions". Technical specifications of processor have been given in Table 2.

Table 2. Technical specifications of processor

Technical specification	
Nominal output power	400 W
Working frequency	24 kHz
Output control	Amplitude 20-100%
Pulse-pulse mode (processor cycle) factor	10%-100% per second

The ultrasonic transducers use electric excitation to generate ultrasound, which is transferred to the sample via various sonotrodes. Sonotrodes are composed of

titanium alloy. The sonotrode with diameter of 3 mm (H3, Dr. Hielscher, GmbH, Germany) was used with UP400S and connected to the processor by an adapter horn (AH22, Dr. Hielscher, GmbH, Germany). The acoustic power density for this tip is 460 W/cm^2 and maximum amplitude is 210 μm.

Pulse control mode (cycle) can be used to expose heat-sensitive sample to high intensity ultrasonic waves. The pulse mode (processor cycle) factor between non-operation and acoustic irradiation can be continuously varied between 0 and 1. The set value equals the acoustic irradiation time in seconds: the difference to one second is the pause time. For example, if the set value is 0.7, this means that the power discharge equals to 0.7 seconds with a pause time of 0.3 seconds.

In this study PPO solution was added to the potassium phosphate buffer (50 mM, pH 6.5) in a glass tube with an inner diameter of 16 mm and a depth of 50 mm. The tip of horn was immersed about 5 mm into 5 ml solution. The ultrasonic amplitude was chosen as 60, 80 and 100% (125, 170 and 210 µm). Sonication was carried out in temperature controlled dry block heater (HBR-48, Daihan Scientific Co. Ltd., Seoul, Korea) at various temperatures ranging 20-60°C with a 10°C increment for 0, 5, 10, 15, 20, 25 and 30 min. The temperature of the solutions was recorded before and after the process. Immediately after inactivation, the tubes were removed and cooled in an ice bath and the residual enzyme activity was measured. These conditions were chosen according to previously reported studies on enzyme inactivation and applicability by the industry considering economical dimension (Kadkhodaee and Povey 2008).

2.4. Fourier Transform Infrared (FTIR) Spectroscopy

In order to determine the conformational change of PPO after inactivation, secondary structure was analyzed by using FTIR spectroscopy. Transmission spectroscopy was applied for determination of protein bands in the samples. "Transmission spectroscopy is the oldest and most straightforward infrared method. This technique

is based upon the absorption of infrared radiation at specific wavelengths as it passes through a sample. It is possible to analyze samples in the liquid, solid or gaseous forms when using this approach". In this method aqueous samples are placed in CaF_2 windows with a spacer, which are put into demountable liquid cell. A typical liquid cell is shown in Figure 7. Other window materials which are not soluble in water can also be used. The spacer is usually made of polytetrafluoroethylene (PTFE, known as 'Teflon') and is available in a variety of thicknesses, hence allowing one cell to be used for various pathlengths (Stuart 2004).
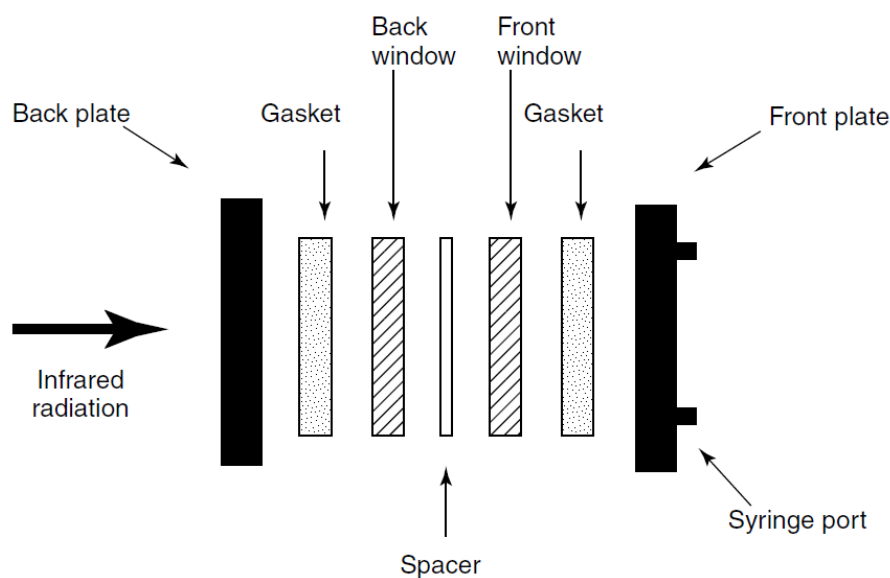
Figure 7. Schematic of a typical liquid cell.

However, these windows have some disadvantages in practice. They are perfectly smooth and after long time periods some leakage occurs in the sample which affects the spectrum. In order to eliminate this problem we have used special windows of different design that consist of flat cover window and a second window (sample window) which has a circular cavity to put into sample at the center of window. Depending upon the path length of the window only a few micro liters are required to fill the sample hole. These windows are fitted into a metal jacket through which heating or cooling liquid from an external bath can circulate. There is no problem in

the usage of these windows for measurements at high temperatures and /or long-time experiments. These windows are shown in Figure 8.
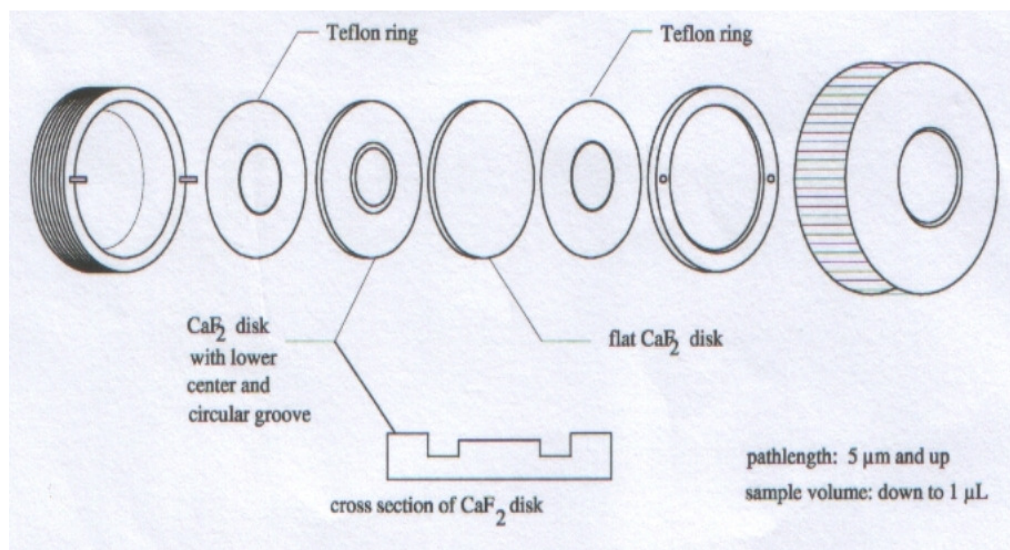
Figure 8. CaF$_2$ disk having a circular cavity in the middle of the bottom window.

Infrared spectra were obtained using Perkin-Elmer Spectrum 100 FTIR spectrometer (Perkin-Elmer Inc., Norwalk, CT, USA) equipped with a MIR TGS detector. The sample compartment was continuously purged with dry air to minimize atmospheric water vapor absorbance, which overlaps in the spectral region of interest, and carbon dioxide interference. To overcome this problem, the spectrum of air was recorded as background and subtracted automatically by using appropriate software.

Mushroom PPO (Sigma) was dissolved in 50 mM phosphate buffer (pH 6.5) to yield a final protein concentration of 70 mg/ml for FTIR measurements. Measurements were performed in H$_2$O buffer for quantitative secondary structure analysis. 10 μl of sample was put between CaF$_2$ windows having a 6 μm path length and then windows was inserted into a cell. In order to control temperature, cell connected to the thermostated circulating water bath. A thermocouple was placed on the outside of the cell to monitor the temperature of the cell. Each spectrum of enzyme solutions and

buffer were collected in the 1200-2800 cm^{-1} region at 25 °C. A total of 400 scans were taken for each interferrogram at 2 cm^{-1} resolution.

For thermal inactivation studies, measurements were performed in D_2O buffer. Prior to infrared experiments, the enzyme was dissolved in 50 mM phosphate buffer (prepared with D_2O). Enzyme solution was allowed to stand 24 h prior to measurement to allow H-D exchange. 10 µl of sample was put between CaF_2 windows having a 50 µm path length and then windows was placed into the system described above. Samples were heated over a linear temperature gradient from 25 to70°C with 2°C intervals and then cooled back to the 25°C. Each spectrum of enzyme solutions and buffer were collected in the 1400-2200 cm^{-1} region. A total of 128 scans were taken for each interferrogram at 2 cm^{-1} resolution. Infrared spectra were recorded continuously.

In this study, measurements were also performed in D_2O buffer for TS inactivation studies. Prior to infrared experiments, the enzyme was dissolved in 50 mM phosphate buffer (prepared with D_2O). Enzyme solution was allowed to stand 24 h prior to measurement to allow H-D exchange. Enzyme solution was put in a glass tube with an inner diameter of 16 mm and a depth of 50 mm. The tip of horn was immersed about 5 mm into 5 ml solution. The ultrasonic amplitude was chosen as 100% (210 µm). Sonication was carried out in temperature controlled dry block heater (HBR-48, Daihan Scientific Co. Ltd., Seoul, Korea) at various temperatures ranging 20-60°C with a 10°C increment for 10 min. The temperature of the solutions was recorded before and after the process. Immediately after inactivation, the tubes were removed and cooled in an ice bath and 10 µl of sample was put between CaF_2 windows having a 50 µm path length and then windows was placed into the system described above. Each spectrum of enzyme solutions and buffer were collected in the 1400-2200 cm^{-1} region. A total of 128 scans were taken for each interferrogram at 2 cm^{-1} resolution.

2.4.1 Data acquisition and spectroscopic analysis

Collections of spectra and data manipulations were carried out using Spectrum 100 software (Perkin-Elmer). Infrared spectra of buffer solution were measured under identical conditions. Each sample was scanned three times and their averages were used for visual and quantitative comparison.

Water is the most frequently used environment for biological systems, which is a strong infrared absorber, in the FTIR studies. It gives strong bands around at 1700 – 1500cm^{-1}, which interferes with the bands of interest arising from functional groups belonging to proteins. As the infrared absorption of water masks protein bands, it is often required to subtract the water bands from the sample spectra by using the appropriate software. So to remove water absorption bands, the spectrum of suspension buffer were subtracted from the spectra of enzyme solution. In the subtraction process the water band located around 2125 cm^{-1} was flattened. Spectrum 100 software (Perkin-Elmer) was used for the subtraction procedure. After subtraction procedure protein bands were obtained.

For the determination of protein secondary structure variations, OPUSNT data collection software (Bruker Optics, Reinstetten, Germany) was used to generate Fourier self-deconvolution and second derivative spectra from amide I band (1700-1600 cm^{-1}). The second derivatives spectra were obtained by applying a Savitzky–Golay algorithm with nine smoothing points and these derivatives vector normalized at 1700-1600 cm^{-1} and then the peak intensities were calculated. The peak minima of the second derivative signals were used, since they correspond to the peak positions of the original absorbance spectra. In the Fourier self-deconvolution, a half bandwidth of 14 cm^{-1} and resolution enhancement factor $k = 2.4$ were used for the absorbance spectra. Deconvolved spectra were fitted with Lorentzian band profiles.

NN analysis of the samples in H$_2$O was applied as described in Severcan et al. (2001). In the Amide I region curve-fitting analysis was used to obtain information

about the changes in the secondary structure of the enzyme during thermal treatment in D_2O. Curve-fitting analysis was performed by using Grams 32 (Galactic Industries, Salem, NH, USA) software. The center positions for each sub-band were determined by second derivative analysis and the shapes of the underlying bands were chosen as Gaussian. The iterations were performed until the correlation was better than 0.995 (Stuart 2004, Haris and Severcan 1999, Severcan and Haris 2003, Garip and Severcan 2010).

2.5. Statistical Analysis

The data were analyzed as a completely randomized design by analysis of variance using Minitab 16 (Minitab Inc.State College, PA). Mean separation was performed by Tukey test at $p < 0.05$ level. Analyses results were the mean with triplicate.

CHAPTER 3

RESULTS AND DISCUSSIONS

3.1. PPO Inactivation

PPO, the main cause of enzymatic browning, is one of the most noticeable enzymes in plants. Enzymatic browning is the result of oxidation of o-diphenols into unstable quinones by PPO enzyme in the presence of molecular oxygen. o-Quinones are highly reactive compounds and react with other phenols and non-phenolic compounds to give brown pigments. These reactions may alter the texture, flavor, color and nutritive value of food products. Therefore, the control of PPO activity is important.

PPO activity can be determined by measuring the rate of substrate disappearance or the rate of product formation. The product formation can be determined spectrophotometrically by measuring the optical density of the colored compounds formed from quinones. The use of spectrophotometer to follow colored compound formation from quinones is the easiest method for the measurement of the reaction rates. Catechol is the most suitable substrate for PPO (Queiroz et al. 2008). The effect of catechol concentration in substrate solution on rate of reaction is shown in Figure 9. According to these results 0.2 M catechol concentration in substrate solution was selected for enzyme activity determination as in indicated in the literature (Sun and Song 2003, Bayındırlı et al. 2006).
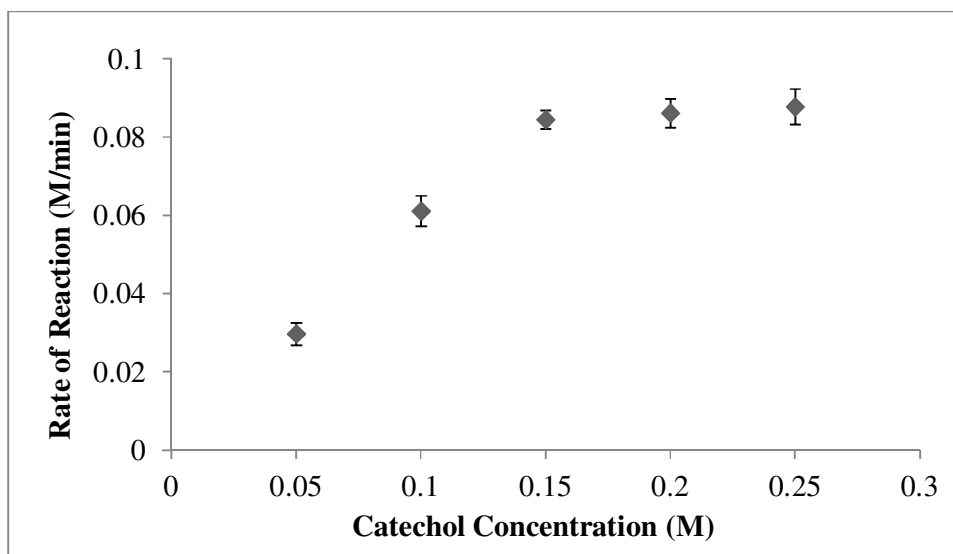
Figure 9. Graph of rate of reaction versus catechol concentrations in substrate solution.

In recent years, ultrasound has been used as an alternative process to thermal treatment for inactivation of enzymes. However, usage of the ultrasound alone may not be sufficient for the inactivation of the food enzymes; combination of ultrasound with mild heat treatment has found to be effective for enzyme inactivation (O`Donnell et al. 2010). Furthermore long-time use of ultrasound alone causes increase in temperature which affects the food quality inversely. Temperature increase during sonication at different ultrasonic power and time is shown in Figure 10.

According to the graph, temperature reaches to 80°C after 30 min ultrasound application. However, it has been reported that PPO is not a heat stable enzyme, and short times is adequate to inactivate PPO at temperatures between 70 and 90°C (O`Donnell et al. 2010). By using dry block heater, the temperature of the enzyme solution was hold as constant during the experiment. Actually, the temperature varied at ±2°C with respect to the average temperature. Therefore, inactivation of PPO was achieved by using TS treatment.
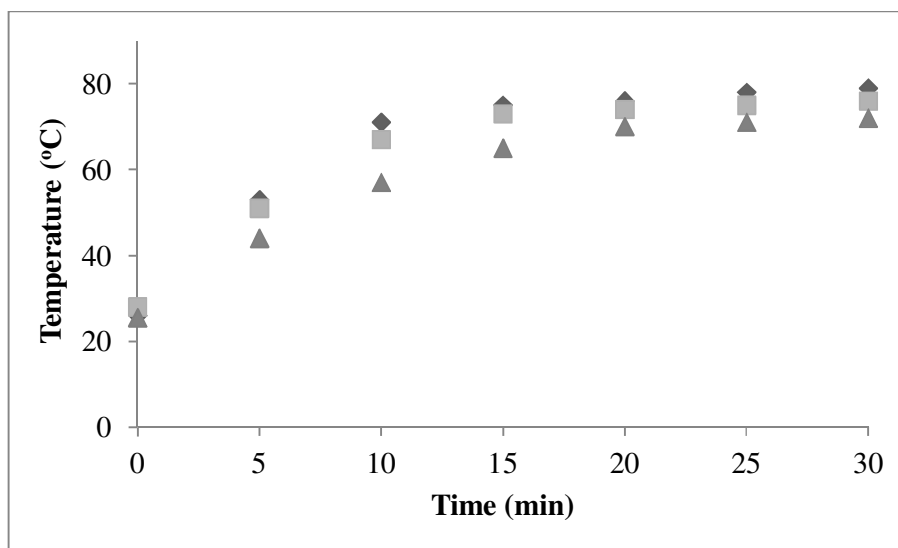
Figure 10. Temperature increase during sonication at 100% (210 µm) (♦), 80% (170 µm) (■) and 60% (125 µm) (▲) ultrasonic powers.

3.1.1. PPO Inactivation during Thermal Treatment

The residual enzyme activity of mushroom PPO after thermal treatment for different time intervals is shown in Figure 11. When stability of mushroom PPO after 30 min exposure to different temperatures was investigated, the enzyme remained fully active up to $40^{o}C$ (data not shown). There was a slight decrease during the period of 30 min at 40°C and activity of enzyme was detected as 89.84 ± 2.70% after 30 min heat treatment at 40 °C. Between $50^{o}C$ and 70°C, higher inactivation was achieved and approximately 99% inactivation was detectable at 70°C for 5 min (Figure 11). Furthermore, no activity was observed over 80°C. Residual enzyme activity after 30 min heat treatment at 50 and $60^{o}C$ were detected as 23.60 ± 1.26% and 0.42 ± 0.03%, respectively. From the graph, it could be seen that the rate of PPO inactivation depended on temperature and increased with increasing temperature and time ($p <$ 0.05). Furthermore, there was a significant interaction ($p < 0.05$) among time and temperature.
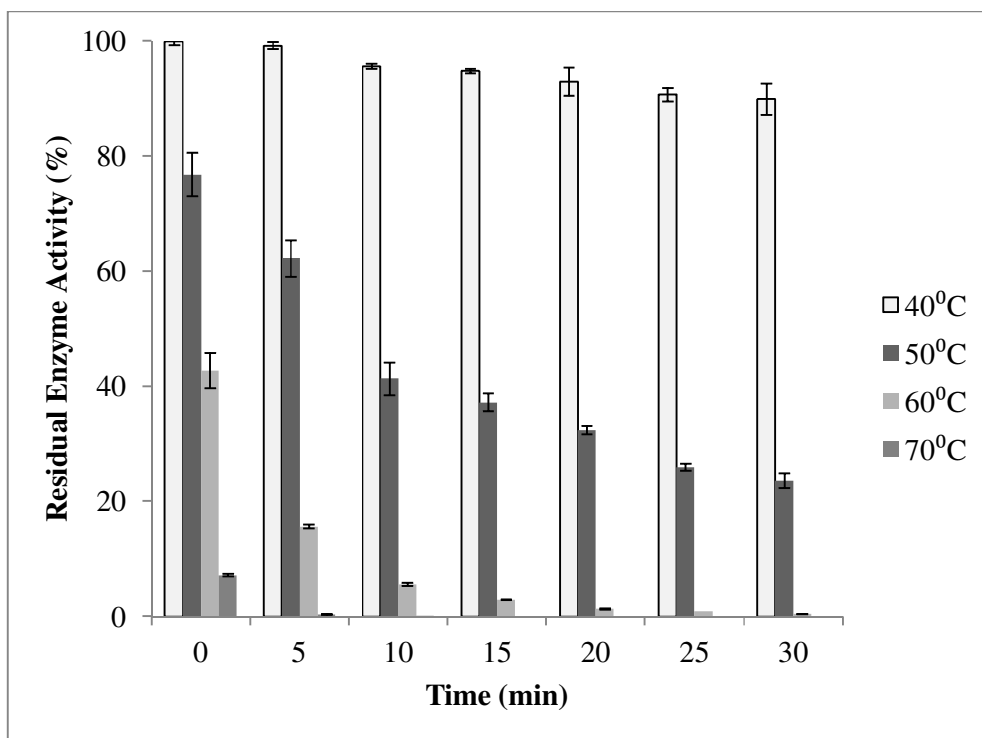
Figure 11. Thermal stability of PPO.

Results found in this study were similar to those found in literature. The mushroom PPO enzyme remained fully active up to 45°C after 10 min exposure to different temperatures and between 45°C and 70°C a gradual decline in activity was observed and above 70°C no activity was detectable (McCord and Kilara 1983). It was reported that mushroom PPO enzyme did not show a considerable inactivation up to 45°C. The considerable inactivation of PPO started above 45°C and accelerated by further increase of the heating temperature. However, the enzyme maintained 23 – 36% of its activity after 30 min at 60°C (Şimşek and Yemenicioğlu 2007). The highest stability of PPO from edible mushroom *Agaricus bisporus* was found in the 30–35°C range, and no remaining activity could be found after incubation of the enzyme at 65°C for 30 min. It was reported that the decline in PPO activity was very drastic at temperatures above 45°C. At 50°C, 50% of PPO activity in mushroom was lost after 30 min of heating, whereas at 55°C more than 80% of the PPO activity was lost (Gouzi et al. 2012).

Cheng et al. (2013) studied the thermal stability of PPO in mushroom during 30 min at temperatures ranging from 30°C to 75°C. The thermal stability of mushroom PPO for 30 min declined as the temperature increased from 30 to 75°C. The decline in the PPO activity was very rapid at temperatures above 50°C. 46% of PPO activity in mushroom extract was lost when heated for 30 min at 55°C, whereas more than 90% of the PPO activity was lost when it was heated for 30 min at 60°C. Furthermore, these results were in agreement with Ionita et al. (2014), who examined thermal inactivation of tyrosinase from A. bisporus in the temperature range 50 – 65°C and found that the thermal treatment caused a gradual decrease in tyrosinase activity.

However, thermostability of PPO from different sources is various. Pineapple PPO activity reduced approximately 60% after exposure to 40 – 60°C for 30 min, residual activity was about 7% after 5 min at 85°C and 1.2% after 5 min at 90°C (Chutintrasri and Noomhorm 2006). In Victoria grape PPO the complete inactivation was reported after 10 min at 70°C (Rapeanu et al. 2006). PPO extracted from strawberry was also thermosensitive. Its activity reduced 50% after 10 min of heating at 55°C and the enzyme was almost completely inactivated after 10 min or thermal treatment at 65°C (Dalmadi et al. 2006).

3.1.2. PPO Inactivation during Thermosonication (TS) Treatment

The residual enzyme activity of PPO after ultrasound treatment at 100, 80 and 60% amplitude at different temperatures is represented in Figure 12, 13 and 14, respectively. The activities of PPO dropped slightly during the period of 30 min at 20°C after ultrasound treatment at 100% amplitude. The maximum inactivation was about 15.38 ± 0.83% after 30 min treatment at 20 °C. In fact, higher PPO inactivation was observed after treatments between 30 and 60 °C with ultrasound compared to the activity in untreated samples. Accordingly, the residual activity was approximately 68.71± 0.78% after inactivation at 30°C for 30 min, 45.08 ± 1.92% after inactivation at 40°C for 30 min and 7.68 ± 0.25% after inactivation at 50°C for 30 min. However, 99% inactivation was achieved at 60°C for 10 min.

Similar trend was also observed for 80 and 60% amplitude ultrasound treatment. After 80% amplitude ultrasound treatment for 30 min, residual enzyme activity was found as 85.91±1.64%, 77.73±0.79%, 57.14±0.75% and 8.51±0.43% for 20, 30, 40 and 50°C, respectively. This inactivation were found as 86.67±1.04%, 79.93±1.62%, 60.94±0.86% and 11.59±0.50% for 20, 30, 40 and 50°C, respectively after 60% amplitude ultrasound treatment for 30 min. However, 99% inactivation was obtained for 15 min for 80% amplitude and for 20 min for 60% amplitude at 60 °C ultrasound treatment.

It could be seen from the graphs, residual enzyme activity decreased with increasing amplitude, time and temperature. Time, temperature and ultrasonic power had a significant effect on ($p < 0.05$) the inactivation of mushroom PPO. Interaction of time and temperature, time and amplitude, temperature and amplitude were significant ($p < 0.05$). Also, there was a significant interaction between time, temperature and ultrasonic power ($p < 0.05$). As a result the residual activities of mushroom PPO decreased significantly ($p < 0.05$) with rise of ultrasonic power, temperature and time.
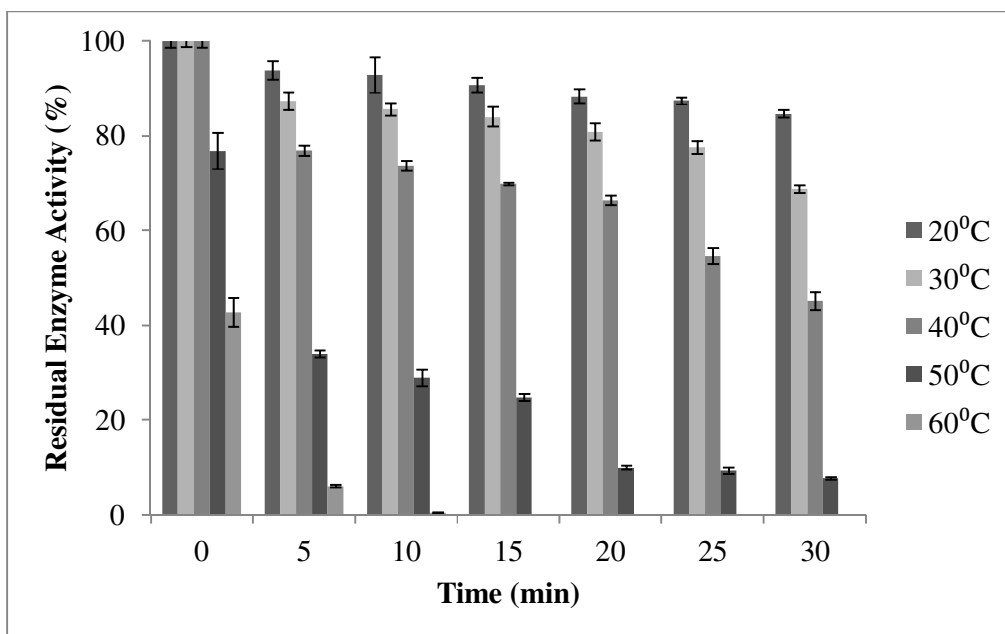
Figure 12. Residual PPO activities after ultrasound treatment at 100% amplitude at different temperatures.
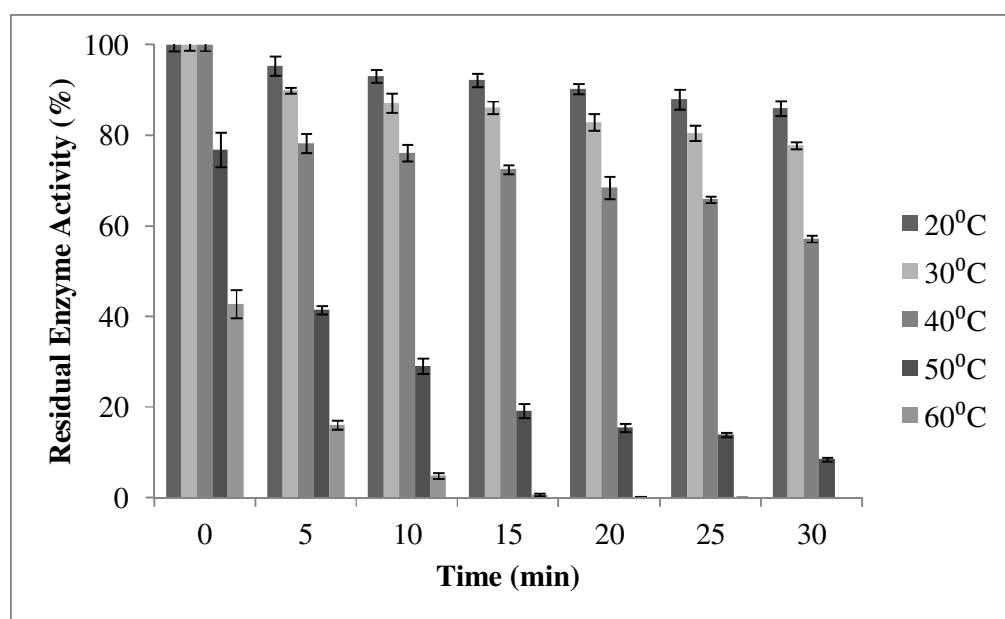
Figure 13. Residual PPO activities after ultrasound treatment at 80% amplitude at different temperatures.
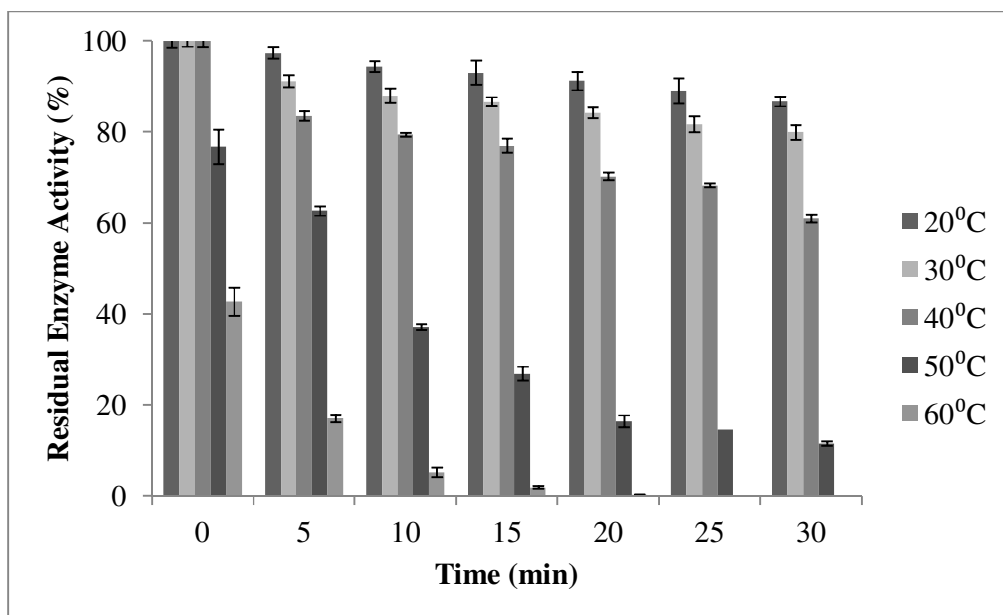
Figure 14. Residual PPO activities after ultrasound treatment at 60% amplitude at different temperatures.

In order to compare the effect of thermal and thermosonication treatment on the activity of PPO enzyme at 60°C, residual enzyme activities (%) were plotted as a function of time (Figure 15). As can be seen from the figure, PPO enzyme was effectively inactivated after ultrasound treatment at 100% amplitude compared to the thermal treatment alone.
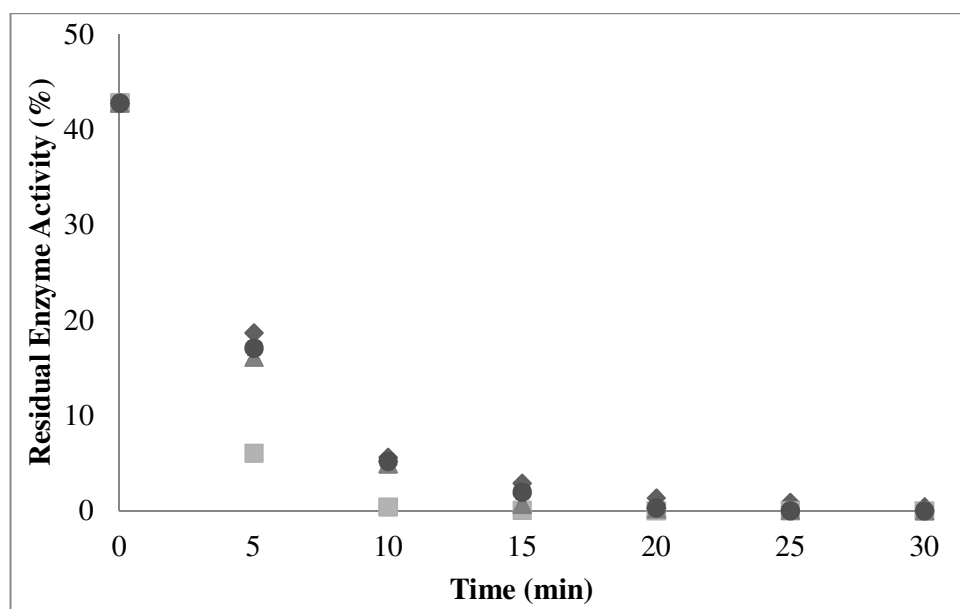
Figure 15. Residual PPO activities after thermal and thermosonic treatments at 60°C ((◆) Thermal treatment, (■) ultrasound treatment at 100% amplitude, (▲) ultrasound treatment at 80% amplitude, and (●) ultrasound treatment at 60% amplitude).

The decimal reduction time (D-value) was calculated and presented in Table 3 in order to evaluate the effect of treatment time. The D-values of PPO treated by thermosonication were found to be less than the D-values obtained from thermal treatment at the same temperature. It can be said that PPO has been found to be sensitive to the ultrasonic waves. The z-values of thermal and TS treatments obtained by plotting the D-value on a log scale as a function of temperature. The temperature was started from 40°C because inactivation of the enzyme was observed after this temperature for thermal treatment. The z-values of thermosonication treatments of 100, 80 and 60 % amplitude were obtained to be 15.11, 15.43 and 14.37°C, respectively. The z-values of thermosonication treatments were higher than the z-value of thermal treatment, which was found as 12.53°C. Similarly, higher z-value (13.8°C) was obtained when inactivation of mushroom PPO was carried out in buffer using thermosonication compared to when inactivation was carried out using thermal treatment (z=10.3°C) (Cheng et al. 2013). This indicates that the heat and ultrasound act synergistically in inactivating the enzymes.

Table 3. D-values of thermal and thermosonication PPO inactivation

Temperature (°C)	D-value of thermal treatment (min)	D-value of thermosonication treatment (min)		
		100 % amp	80 % amp	60 % amp
20	-	208.33	217.39	220.54
30	-	99	136.99	149.25
40	263.15	44.05	65.79	84.74
50	23.41	12.16	14.88	16.92
60	6.66	2.09	3.33	3.44
70	1.097	-	-	-
z value (°C)	12.53	15.11	15.43	14.37

Enzyme inactivation by ultrasound is widely reported in literature and TS treatment was found to be better than thermal treatment for the inactivation of different types of enzymes such as pectinmethylesterase, PPO, lipoxygenases and peroxidases responsible for deterioration of fruit & vegetable juice.

The combined effect of heat and ultrasonic waves at 4 kg/cm^2 of absolute pressure for the inactivation of mushroom PPO were studied (Lopez et al. 1994). Heat resistance at 70.7°C and MTS inactivation at an absolute pressure of 4 kg/cm^2 and ultrasound amplitude of 35 µm at 37 and 70.7°C of mushroom PPO was compared. Synergistic effect of heat and ultrasonic waves on PPO inactivation was reported. Furthermore, effect of ultrasound amplitude on mushroom PPO inactivation at 4 kg/cm^2 of absolute pressure at 60°C were investigated. It was reported that the greater the amplitude, the higher the efficiency. A linear decrease in log D values for an increase in ultrasound amplitude level over the range 35-145µm was observed. They reported that heat or pressure assisted ultrasonic processing of juice can

substantially reduce enzyme resistance and the heat treatment required for inactivation.

The effect of thermal and thermosonic treatments on the inactivation kinetics of polyphenol oxidase (PPO) in mushroom (*Agaricus bisporus*) in 55 – 75°C temperature range was studied for 0-30 min (Cheng et al. 2013). The ultrasound treatments were carried out at 25 kHz frequency and 50% of the maximal equipment power with pulse durations of 5 s on and 5 s off at temperatures ranging from 55°C to 75°C for 0-30 min. It was reported that mushroom PPO in crude enzyme extract was inactivated relatively slowly at 55°C, while at temperatures higher than 60°C, the inactivation rate of mushroom PPO increased dramatically. It was found that residual mushroom PPO activity was only about 1.0% at 60°C after thermosonication treatment for 15 min, whereas 3 min long thermosonication at 75°C completely inactivated the enzyme. The D values of PPO decreased by 1.3 - 3 times during thermosonic inactivation compared to the D values of PPO during thermal inactivation at the same temperature range. It was concluded that the inactivating effect of combined ultrasound and heat was found to synergistically enhance the inactivation kinetics of PPO.

A similar result was also observed for lemon pectinesterase. The activities of PE dropped slightly during the period of 1 hour in the temperature range between 40 and 50°C. After heating at 50°C without the ultrasound the residual activity was only 30% decreased whereas with the ultrasonic treatment for 63 min, the residual activity was 83% decreased (Kuldiloke et al. 2007). The TS treatment was also found to be better than the heat blanching process for the inactivation watercress peroxidase, known as heat resistance enzyme (Cruz et al. 2006). In another study tomato juice was subjected to TS treatment and reduced PME activity by 90% at 60 °C, 65 °C and 70 °C for 41.8, 11.7 and 4.3 min exposure, respectively (Wu et al. 2008).

In a recent study, fresh apple juice was thermosonicated using ultrasound in-bath (25 kHz, 30 min, 0.06W/cm^{3}) and ultrasound with-probe sonicator (20 kHz, 5 and 10

min, 0.30W/cm^3) at 20, 40 and 60 °C for inactivation of enzymes (polyphenolase, peroxidase and pectinmethylesterase). It was reported that the inactivation of all the enzymes was more pronounced for apple juice treated with-probe compared to those treated in-bath type sonicator and the highest inactivation of enzymes was obtained at 60 °C for 10 min. residual activities of PPO treated with probe at 20 °C for 5 and 10 min was found as 98.16 and 97.04%, respectively. A bit higher reduction was observed in activity of PPO at 40 °C, residual activities for 5 and 10 min at 40 °C was found as 61 and 53%, respectively. Considerable reduction was reported in activity of PPO at 60 °C, residual activities for 5 and 10 min at 60 °C was found as 21.15 and 6.15%, respectively. These results were accordance with those reported in the study (Abid et al. 2014).

3.2. FTIR Studies

3.2.1. Infrared Spectroscopy of PPO in H$_2$O

In the present study, secondary structure of the enzyme was analyzed by using FTIR spectroscopy. For this purpose enzyme solution and buffer were placed in CaF$_2$ windows which were inserted into demountable liquid cell. The spectrum of air was recorded as background and subtracted automatically from these spectra. The spectrum of buffer was subtracted from the spectra of enzyme solution to remove water absorption bands. In the subtraction process the water band located around 2125 cm^{-1} was flattened. After subtraction procedure protein bands were obtained. In order to get best spectrum for protein bands optimization was applied. At the end of the optimization 400 scan and 2 cm^{-1} resolution was chosen. Spectrum of enzyme solution, buffer and subtracted spectrum of the protein bands are shown in Figure 16.
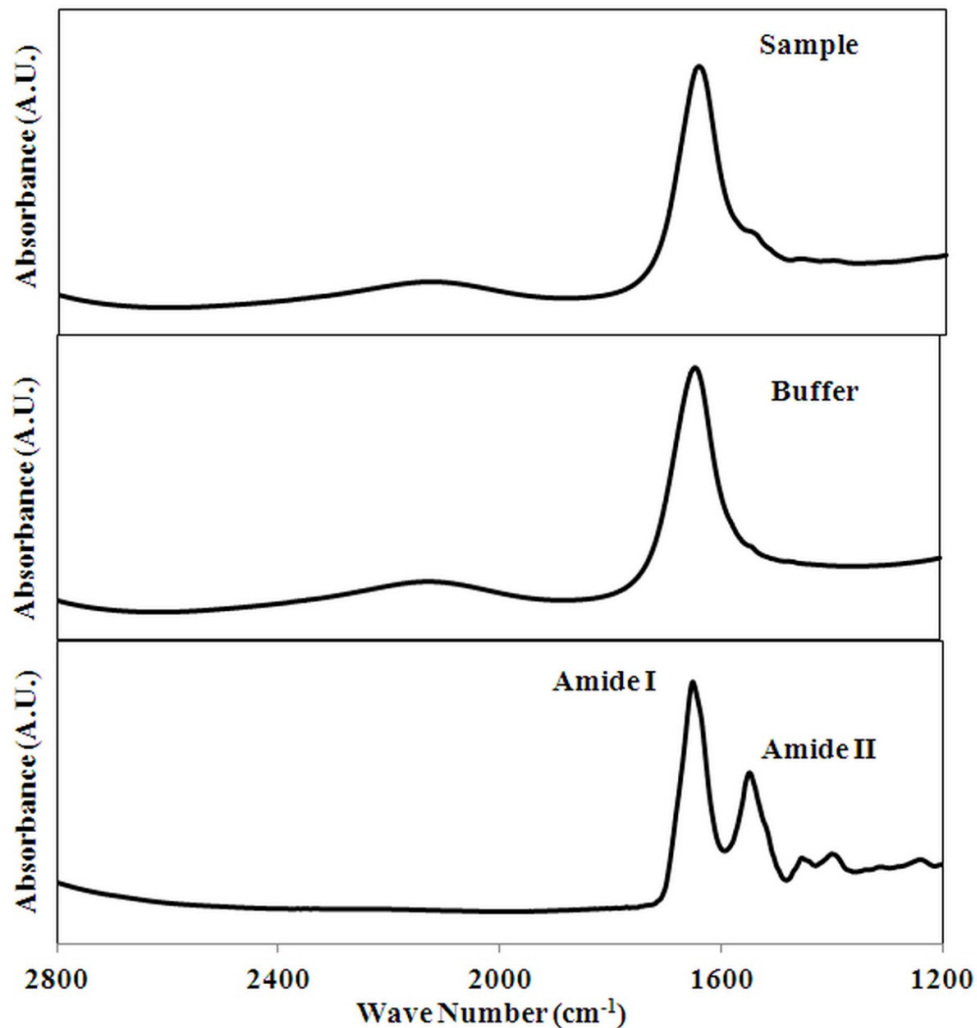
Figure 16. Spectrum of enzyme solution, buffer and subtracted spectrum of protein bands.

Absorbance (1750 – 1500 cm^{-1}), Fourier self-deconvolution (1750 – 1500 cm^{-1}), and second-derivative (1700 – 1600 cm^{-1}) FTIR spectrum of PPO in H$_2$O buffer at 25 °C are shown in Figure 17. In the absorbance spectrum, the peak at 1653 cm^{-1} is assigned as amide I band which arises from mainly amide C=O stretching (80%) frequencies of the protein backbone and the peak at 1550 cm^{-1} is assigned as amide II band which is due to N-H bending (60%) and C-N stretching (40%) vibrations of the peptide backbone (Stuart 2004, Haris and Severcan 1999).

The position of the amide II band is sensitive to deuteration, shifting from around 1550 cm^{-1} to a wavenumber of 1450 cm^{-1}. The amide II band of the deuterated protein overlaps with the H–O–D bending vibration, so making it difficult to obtain information about the conformation of this band. However, the remainder of the amide II band at 1550 cm^{-1} may provide information about the accessibility of solvent to the polypeptide backbone due to the contribution of the NH bending vibration to the amide II. The most useful infrared band for the analysis of the secondary structure of proteins in aqueous media is the amide I band, occurring between approximately 1700 and 1600 cm^{-1}. Proteins generally contain a variety of domains containing polypeptide fragments in different conformations. As a consequence, the observed amide I band is usually a complex composite, consisting of a number of overlapping component bands representing helices, β-structures, turns and random structures (Stuart 2004).

Analysis of amide I band (1700-1600 cm^{-1}) by using second derivative and Fourier self-deconvolution techniques gives qualitative information on the secondary structure of a protein (Haris and Severcan 1999). The deconvoluted spectra revealed that the major amide I band at 1653 cm^{-1} was due to α-helix structure. The peak located at 1676 cm^{-1} was assigned to β-turn structure. The band at 1636 cm^{-1} was often assigned to β-sheet structure. The peak at located around 1617 cm^{-1} was due to aggregated β-sheet structure. The amide II which was located at 1548 cm^{-1} could not be readily assigned to any particular secondary structure. This band was used to monitor hydrogen-deuterium exchange (Severcan and Haris 2003, Murayama and Tomida 2004).

Quantitative secondary structure analysis of PPO in H_2O buffer was carried out by using NN analysis method. According to the NN analysis, PPO contained 42.33 ± 3.06 % α-helix structure, 21.33 ± 4.73 % β-sheet structure, 19.67 ± 1.15 % turns and 16.67 ± 1.53 % random coil structure, demonstrating that PPO enzyme was α-helix dominating enzyme. This finding agreed with that reported by Tse et al. (1997) and Ionita et al. (2014).
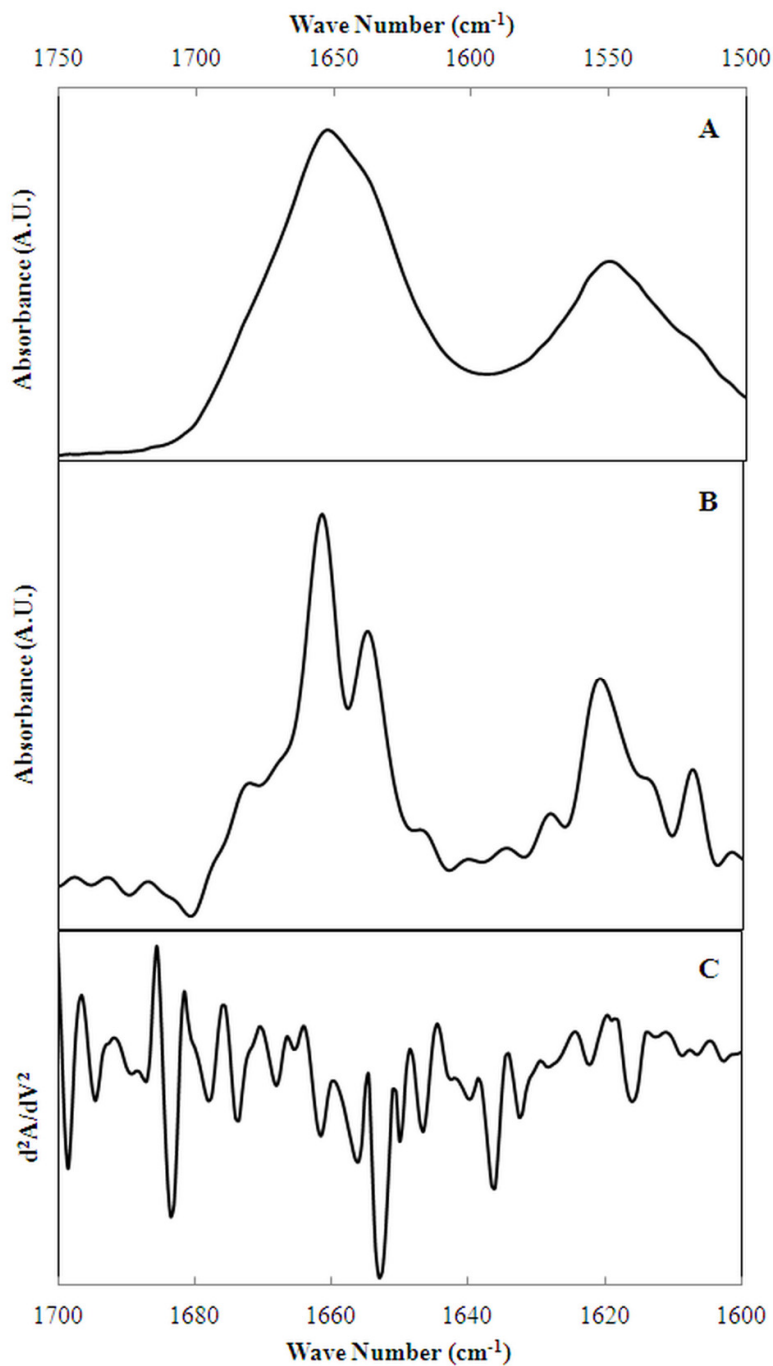
Figure 17. (A) Absorbance (1750 – 1500 cm^{-1}), (B) Fourier self-deconvolution (1750 – 1500 cm^{-1}), and (C) second-derivative (1700 – 1600 cm^{-1}) FTIR spectrum of PPO in H$_2$O buffer at 25 °C.

3.2.2. Infrared Spectroscopy of PPO in D_2O

In order to determine the secondary structure and conformational changes of mushroom PPO during thermal and thermosonication treatment, measurements were performed in D_2O buffer. Figure 18 displays absorbance, Fourier self-deconvolution, and second-derivative FTIR spectrum of PPO in D_2O buffer at 25 ℃. It could be seen from the absorbance spectrum of PPO that the amide II band at 1550 cm^{-1}, seen for PPO in H_2O buffer, disappeared and shifted to the 1455 cm^{-1}, suggesting that hydrogen-deuterium exchange occurred. The bands observed in D_2O were in good agreement with the bands observed in H_2O for both Fourier self-deconvolution and second derivative analysis.

According to the Fourier self-deconvolution analysis the band located at 1652 cm^{-1} is due to α-helix structure. The peak located at 1673 cm^{-1} is assigned to β-turn structure. The band at 1635 cm^{-1} is assigned to β-sheet structure. The peak at located around 1616 cm^{-1} is due to aggregated β-sheet structure. There was a shift towards lower frequencies due to the hydrogen-deuterium exchange in the sub bands.
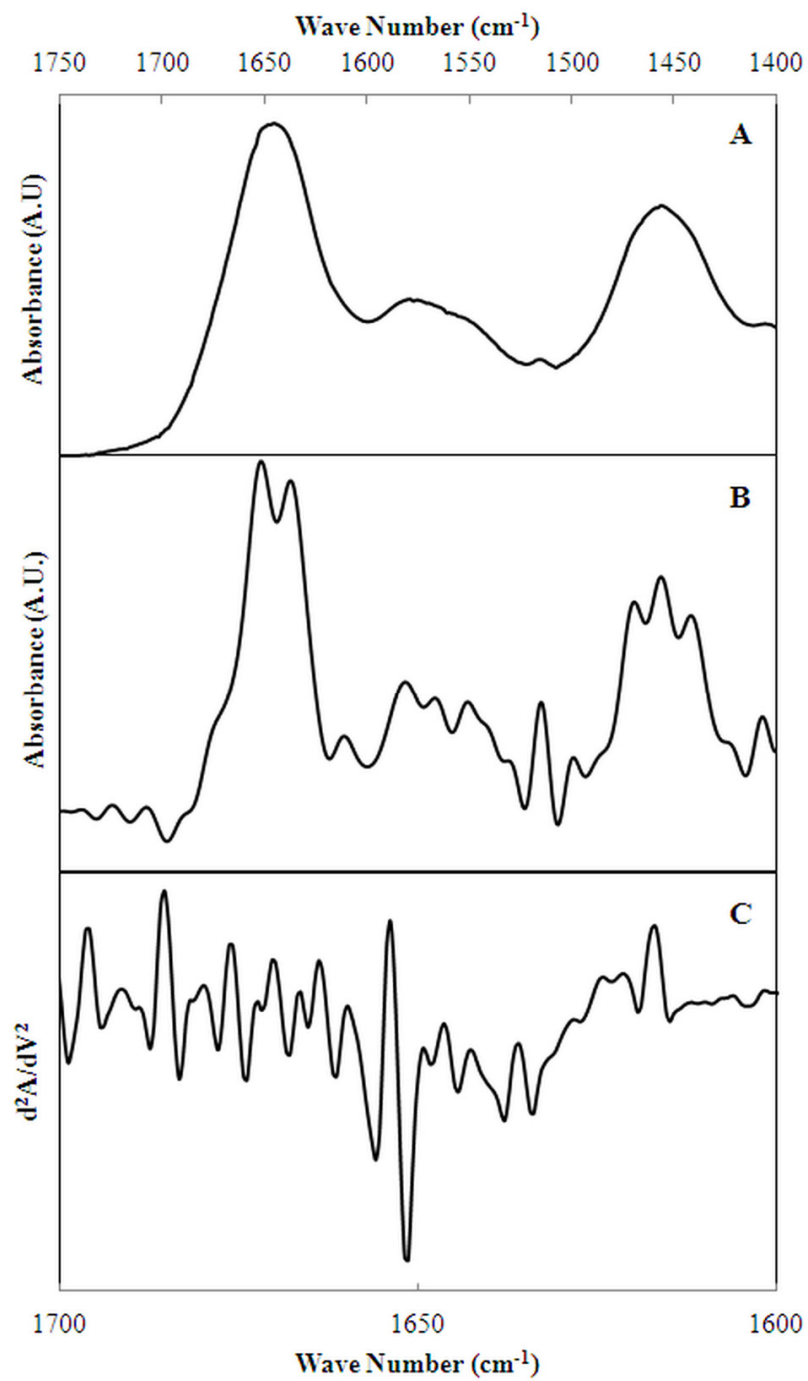
Figure 18. (A) Absorbance (1750 – 1400 cm^{-1}), (B) Fourier self-deconvolution (1750 – 1400 cm^{-1}), and (C) second-derivative (1700 – 1600 cm^{-1}) FTIR spectrum of PPO in D$_2$O buffer at 25 ℃.

3.2.3. Effect of heat treatment on mushroom PPO enzyme

Representative absorbance spectra of PPO in the 1750 – 1400 cm^{-1} region recorded at different temperatures are shown in Figure 19. It was observed that the intensity of amide I band decreased as the temperature increased between 25 – 70 ℃. This indicates that there is a change in the secondary structure of the enzyme. However, no change was observed for the spectral patterns between 70 – 80 ℃ (data not shown). The FTIR spectrum above 70 ℃ and that at 25 ℃ after cooling were very similar to each other, stating complete inactivation of the PPO over 70 ℃.
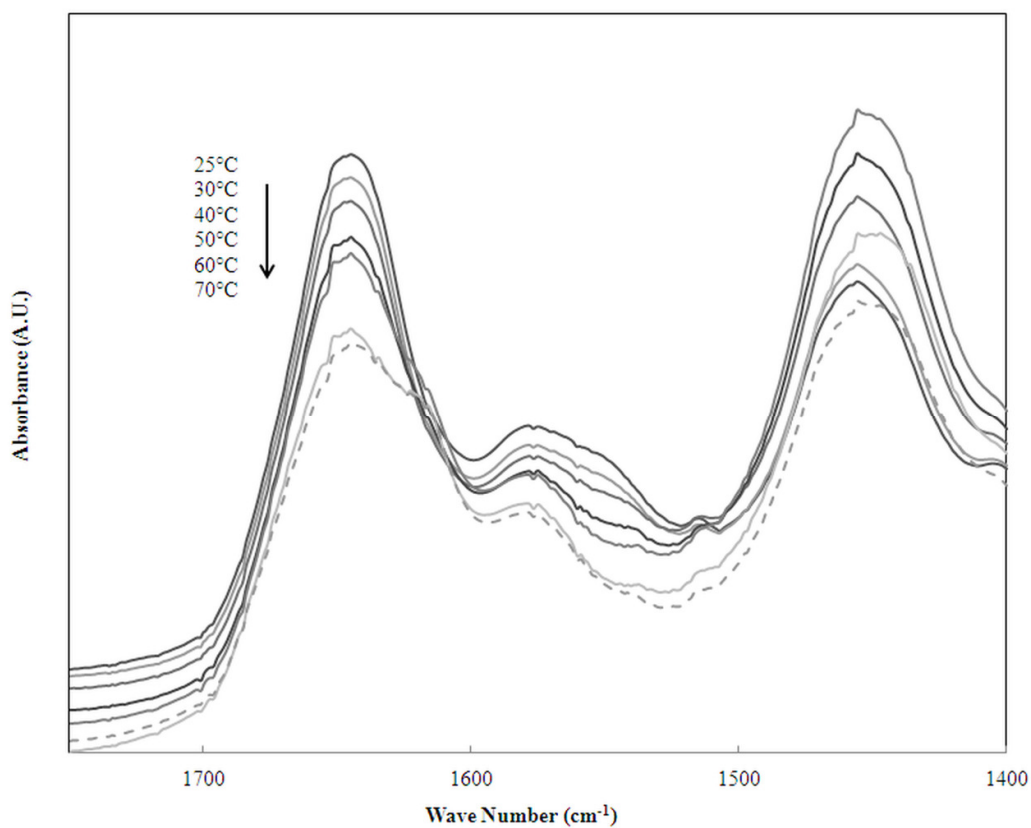
Figure 19. Representative absorbance spectra of PPO in D$_2$O buffer over a temperature range of 25-70 ℃ (solid lines) and spectrum of the PPO measured at 25 ℃ after cooling from 70 ℃ (dotted line).

To explore the temperature induced changes in secondary structure of PPO in detail, Fourier self-deconvolution techniques applied to the FTIR spectra. Figure 20 presents the representative deconvolved spectra of PPO solution in the 1700 – 1600 cm^{-1} region measured between temperature range of 25 – 70 ℃ and at 25 ℃ after cooling. According to the deconvolved FTIR spectra of PPO, there was little change in the temperature range of 25 – 40 ℃. Marked spectral changes were noted after this temperature and additional new bands due to aggregated β-sheet structures appeared at 1683 and 1616 cm^{-1}. These bands were detected when proteins are denatured (Severcan and Haris 2003). The intensity of these bands increased with the increasing temperature. When temperature was lowered back to 25 ℃, from 70 ℃, these bands were still observed, indicating an irreversible change in the structure of PPO. Moreover, intensity of α-helix and β-sheet structure decreased and shifted to the lower values while the temperature increased up to 70 ℃. These observations indicated the loss of secondary structure of PPO during the thermal treatment.
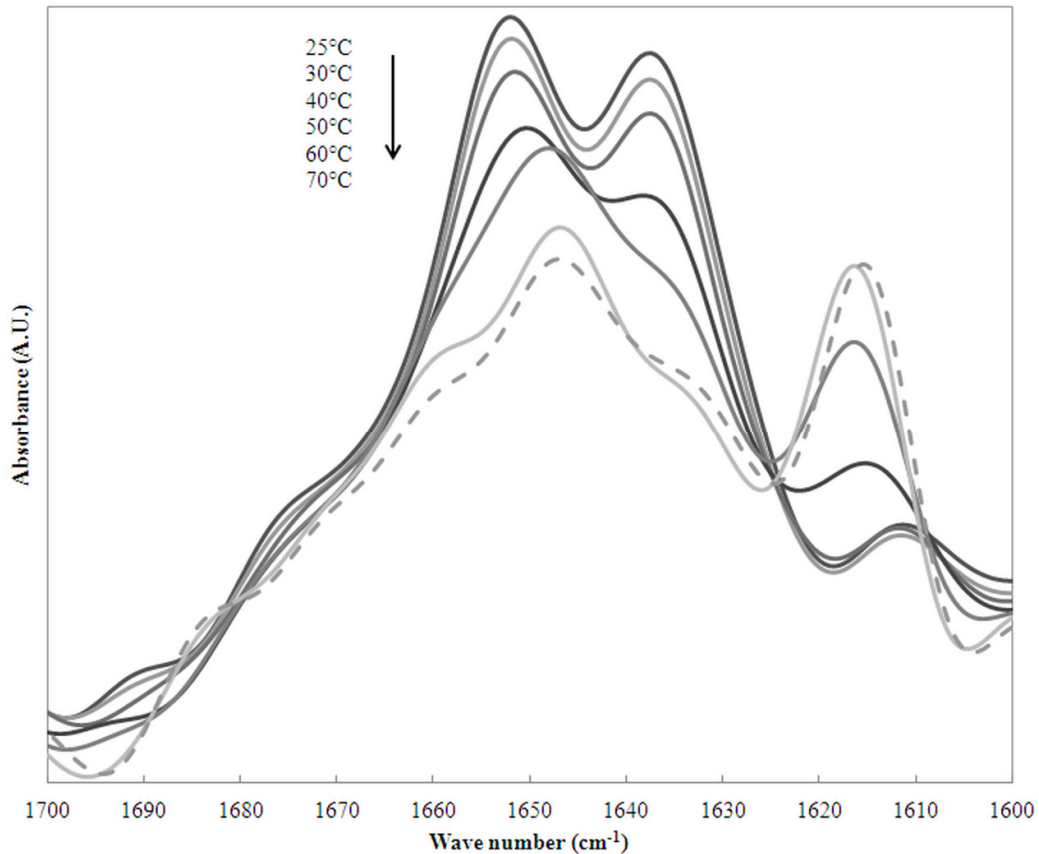
Figure 20. Representative Fourier self-deconvolution spectra of PPO in D_2O buffer over a temperature range of 25 – 70 ℃ (solid lines) and spectrum of the PPO measured at 25 ℃ after cooling from 70 ℃ (dotted line).

According to the X-ray analysis, mushroom tyrosinase is a tetrameric protein composed of two subunits (H and L). H subunit is the domain of the enzyme and containes 13 α-helices, eight mostly short β-strands and many loops in domain. The active site of the enzyme is made up a bundle of four helices in the center of the domain. It is also reported that the L subunit consists of 12 antiparallel β-strands assembled in a cylindrical barrel of six 2-stranded sheets and is not involved in the activation mechanism of the enzyme (Ismaya et al. 2011). As stated in X-ray analysis, reduction in the α-helix affects the active site of the enzyme and caused structural deterioration.

56

The intensities of the amide I band and its components were plotted as a function of temperature in order to estimate the thermal unfolding of PPO more precisely (Figure 21). As stated previously, the intensity of the 1652, 1635 cm^{-1} band decreased as the temperature increased and multistep transition was represented for these bands. In both cases first transition was observed at 36 ℃ and the higher transition occurred at 64 ℃. Intensity profile of the band at 1652 cm^{-1} indicated that α-helix structure was gradually lost up to 64 ℃. However, α-helix structure change occurred sharply in the temperature range 64 – 70 ℃. Similar trend was also observed for the amide I band change, showing that α-helix structure was the main secondary structure component of the PPO, agreed with the NN analysis.

Simultaneously, the intensity of the aggregation band at 1616 cm^{-1} increased with the increasing temperature. The band located at 1616 cm^{-1} firstly appeared at the temperature around 42 ℃. The intensity of the band linearly increased up to 64 ℃ and no significant change was observed after this temperature. Similarly, Tse et al. (1997) found that the secondary structure began to change above 40 ℃ and a new band at 1616 cm^{-1} appeared at 45 ℃ for mushroom tyrosinase.
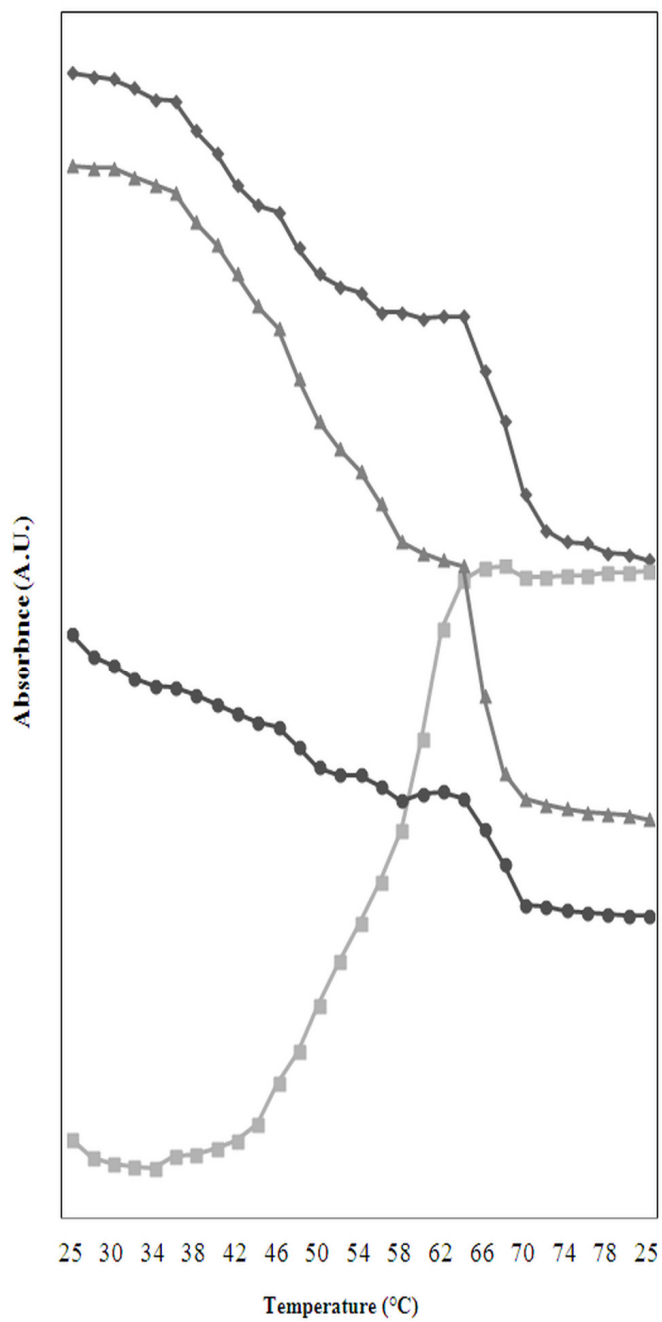
Figure 21. A plot of the temperature induced changes in the intensity of the amide I and its components for PPO during thermal treatment (($\blacklozenge$) 1652 cm^{-1}, ($\blacksquare$) 1616 cm^{-1}, ($\blacktriangle$) 1635 cm^{-1}, and ($\bullet$) amide I).

Using the intensity profiles, transition temperature (T_m) for the different amide I components was determined and represented in Table 4. The T_m values for α-helix, β-sheet, aggregated β-sheet structure and amide I band were determined as around 55 ºC. This value was very close to that reported by McCord and Kilara (1983) and Weemaes et al. (1997) whom found T_m value as 54 ºC and 51.8 ºC, respectively.

Table 4. Transition Temperatures (Tm) for different amide I components for PPO during thermal treatment.

Structure	Amide I band (cm^{-1})	T_m value (ºC)
α-helix	1652	54.72
β-sheet	1635	53.5
Aggregated β-sheet	1616	57.07
Amide I	1653	53

3.2.4. Curve-fitting analysis of PPO during Thermal Treatment

In order to determine secondary structural change during thermal treatment in D_2O curve-fitting analysis was applied to the Amide I region (1700 – 1600 cm^{-1}). The contribution of each component band to the amide I band is shown in Figure 22 for two different temperatures (25 and 70 ºC). The bands at 1652 cm^{-1} due to the α-helix and that at 1635 cm^{-1} due to the β-sheet structure became weaker as temperature increases from 25 to 70 ºC, whereas other bands due to the aggregated β-sheet (1683 and 1616 cm^{-1}), turns (1676 cm^{-1}) and random coil (1640 cm^{-1}) structures became much stronger at 70ºC.
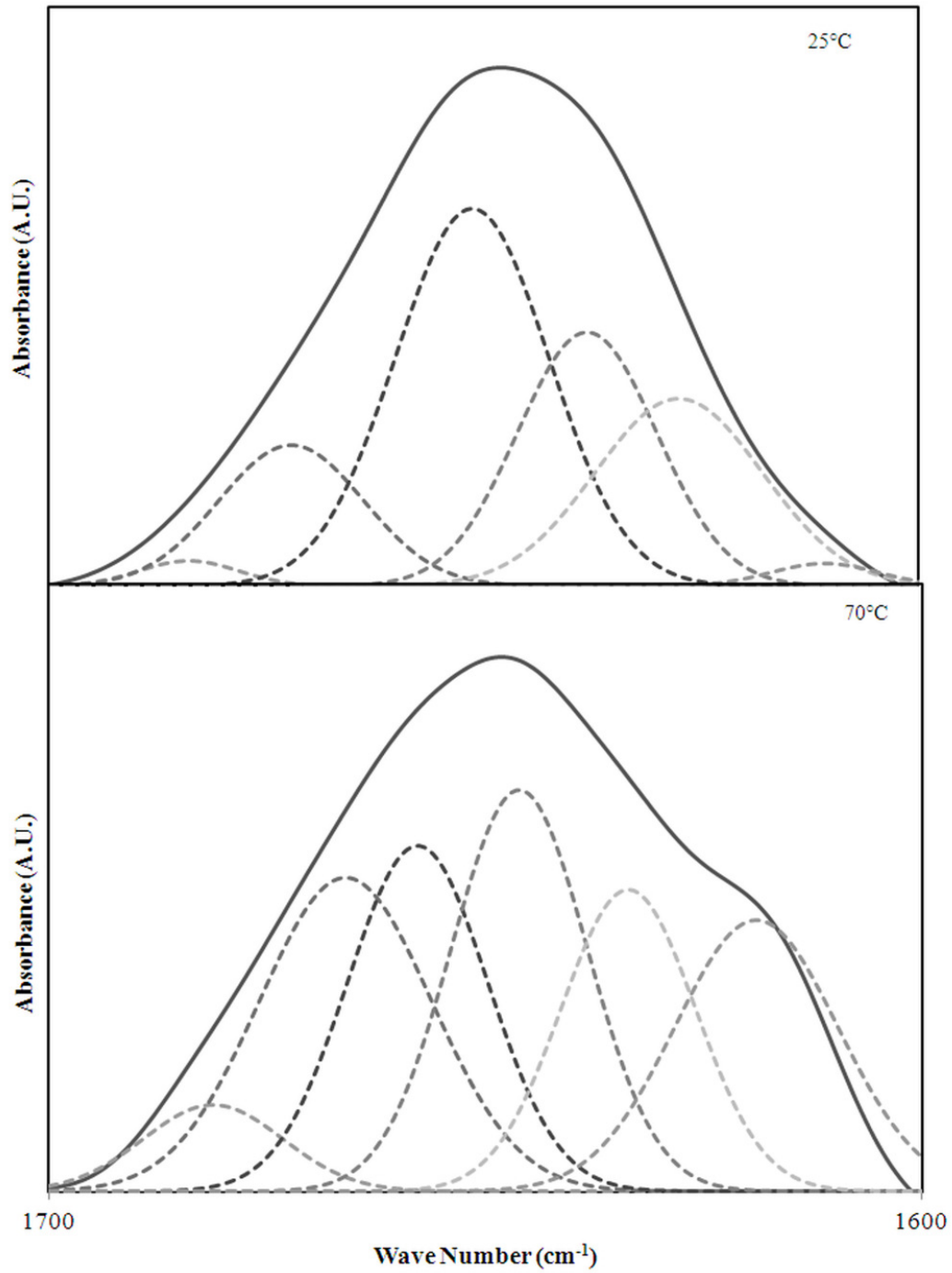
Figure 22. Curve-fitting analysis of amide I band (1700 – 1600 cm^{-1}) of PPO during thermal treatment.

Secondary structural change (%) of PPO during thermal treatment estimated by curve-fitting analysis is shown in Table 5. According to the curve-fitting analysis, PPO contained 38.87 ± 0.02 % α-helix, 27.91 ± 0.02 % β-sheet, 14.93 ± 0.01 % β-turn, 15.01 ± 0.01 % random coil and 3.27 ± 0.06 % aggregated β-sheet structures in untreated sample. This result was accordance with the NN result which indicated that PPO was α-helix dominating enzyme. Previous circular dichroism (CD) studies reported values of 35.3 % (Liu et al. 2013), 35.7 % (Yi et al. 2012) and 41.3 % (Liu et al. 2009) for α-helix content of PPO. α-helix content decreased from 38.87 ± 0.02 % to 19.40 ± 0.21 % ($p < 0.05$), β-sheet content decreased from 27.91 ± 0.02 % to 15.88 ± 0.02 % ($p < 0.05$) whereas β-turn, random coil and aggregated β-sheet structures increased up to 21.93 ± 0.14, 22.47 ± 0.60 and 20.31 ± 0.27 %, respectively ($p < 0.05$).

Table 5. Secondary structure change (%) of PPO estimated by curve-fitting during thermal treatment.

Temperature (ºC)	α-helix	β-sheet	β-turn	Random coil	Aggregated β-sheets
25	38.87 ± 0.02	27.91 ± 0.02	14.93 ± 0.01	15.01 ± 0.01	3.27 ± 0.06
30	35.68 ±0.06	25.14 ± 0.13	14.74 ± 0.02	19.94 ± 0.03	4.50 ± 0.01
40	26.91 ± 0.01	22.83 ± 0.01	18.07 ± 0.01	21.92 ± 0.01	10.28 ± 0.04
50	25.42 ± 0.10	19.50 ± 0.33	16.81 ± 0.07	22.22 ± 0.09	16.05 ± 0.07
60	24.01 ±0.18	18.24 ± 0.14	17.67 ± 0.13	21.20 ± 0.16	18.88 ± 0.60
70	19.41 ±0.16	16.25 ± 0.14	21.68 ± 0.18	22.48 ± 0.65	20.19 ± 0.17
25 (after cooling from 70ºC)	19.40 ± 0.21	15.88 ± 0.02	21.93 ± 0.14	22.47 ± 0.60	20.31 ± 0.27

Graphical representation of the change in the secondary structure components is represented in Figure 23. This representation indicated that α-helix and β-sheet structures were lost as the temperature increase with the formation of aggregated β-sheets and the increase in the turns and disorder structure (1640 cm^{-1}).
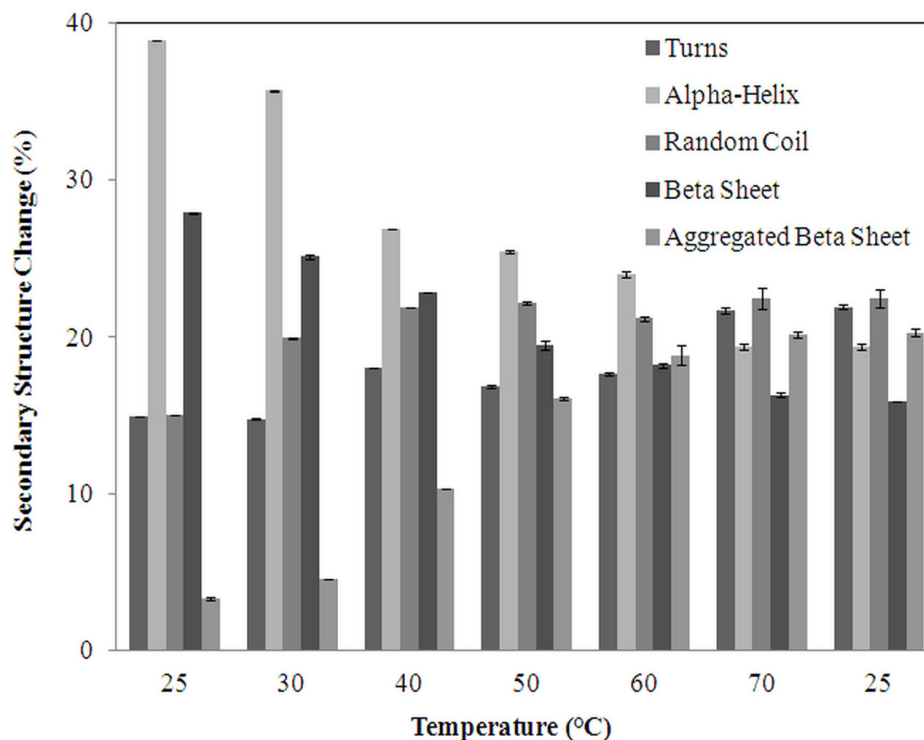
Figure 23. Graph of secondary structure change (%) of PPO according to the curve-fitting analysis during thermal treatment.

3.2.5. Effect of Thermosonication (TS) treatment on mushroom PPO enzyme

Representative absorbance spectra of PPO in the $1750 - 1400$ cm^{-1} region recorded at different temperatures during ultrasound treatment are displayed in Figure 24. It was observed that absorbance spectra of PPO at 25 ℃ and 100% amplitude at 20 ℃ ultrasound treatment were similar in terms of amide I band and the intensity of amide I band decreased as the temperature increased between at $20 - 60$ ℃ at 100% amplitude ultrasound treatments. This indicated that there was a change in the secondary structure of the enzyme during TS treatment. However, no change was observed for the spectral patterns between the FTIR spectrum at 60 ℃ ultrasound treatment and that at 25 ℃ after cooling from 60 ℃ ultrasound treatment, stating complete inactivation of the PPO after 60 ℃ ultrasound treatment.
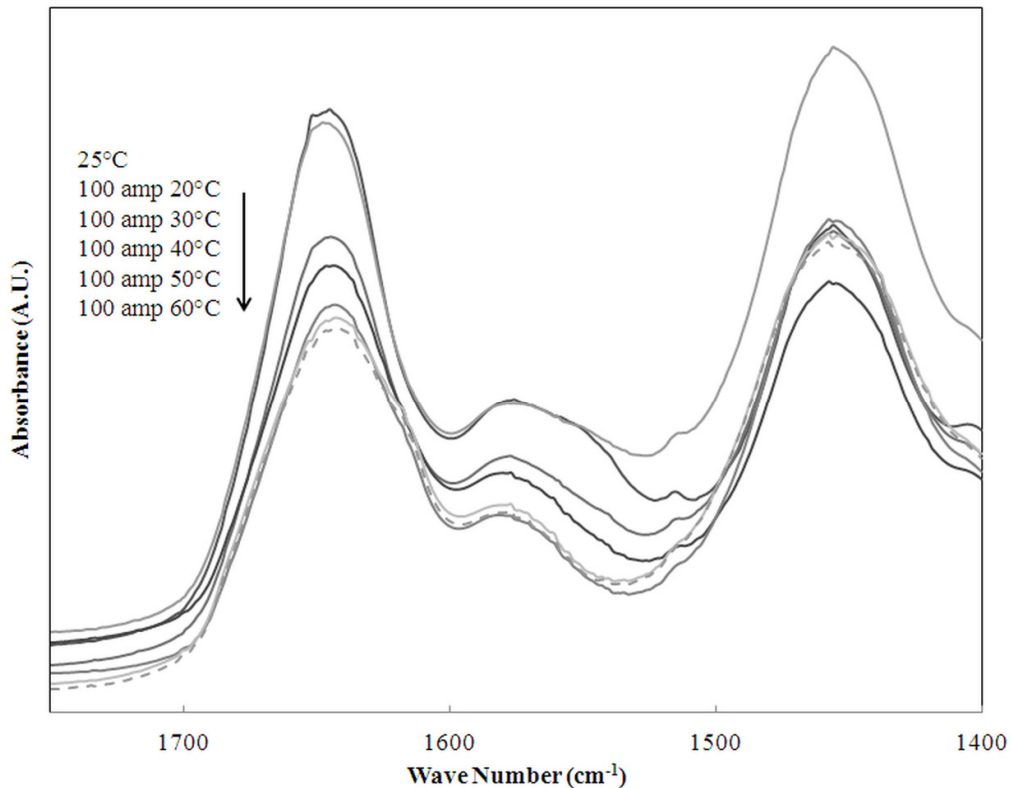
Figure 24. Representative absorbance spectra of PPO in D$_2$O buffer recorded at different temperatures during ultrasound treatment (solid lines) and spectrum of the PPO measured at 25 °C after cooling from 100% amplitude 60 °C (dotted line).

Fourier self-deconvolution of the FTIR spectra was obtained in order to explore the TS induced changes in secondary structure of PPO in detail. Figure 25 presents the representative deconvolved spectra of PPO solution in the 1700 – 1600 cm^{-1} region measured at different temperatures during ultrasound treatment and at 25 °C after cooling from 100% amplitude 60 °C. Deconvolved FTIR spectra of PPO at 100% amplitude 20 °C did not change too much according to that at 25 °C. After this TS treatment, marked spectral changes were noted. Additional new bands due to aggregated β-sheet structures became evident at 1682 and 1616 cm^{-1} after 100% amplitude 40 °C, indicating protein denaturation (Severcan and Haris 2003). The intensities of these bands increased while the temperature increased. When temperature was lowered back to 25 °C, from 100% amplitude 60 °C, these bands

were still observed, indicating an irreversible change in the structure of PPO. The intensities of α-helix and β-sheet structure decreased while the temperature increased up to 60 ºC during TS treatment. Furthermore, the bands at 1640 cm^{-1} due to random coil and at 1670 cm^{-1} due to turns became apparent at 100% amplitude 60 ºC, demonstrating increase in unordered structures. These observations indicated the loss of secondary structure of PPO during the TS treatment and mechanism of enzyme inactivation for TS was different that for temperature.

Similarly, secondary structural components, especially β-sheet, of α-amylase, papain and pepsin were significantly influenced by ultrasound (Yu et al. 2014). The secondary structure of six different proteins (cytochrome, lysozyme, myoglobin, bovine serum albumin, trypsinogen, and α-chymotrypsinogen A) was affected from ultrasound and it was reported that the free radicals, produced by water sonolysis, have an important role in the changes of structural order (Marchioni et al. 2009).
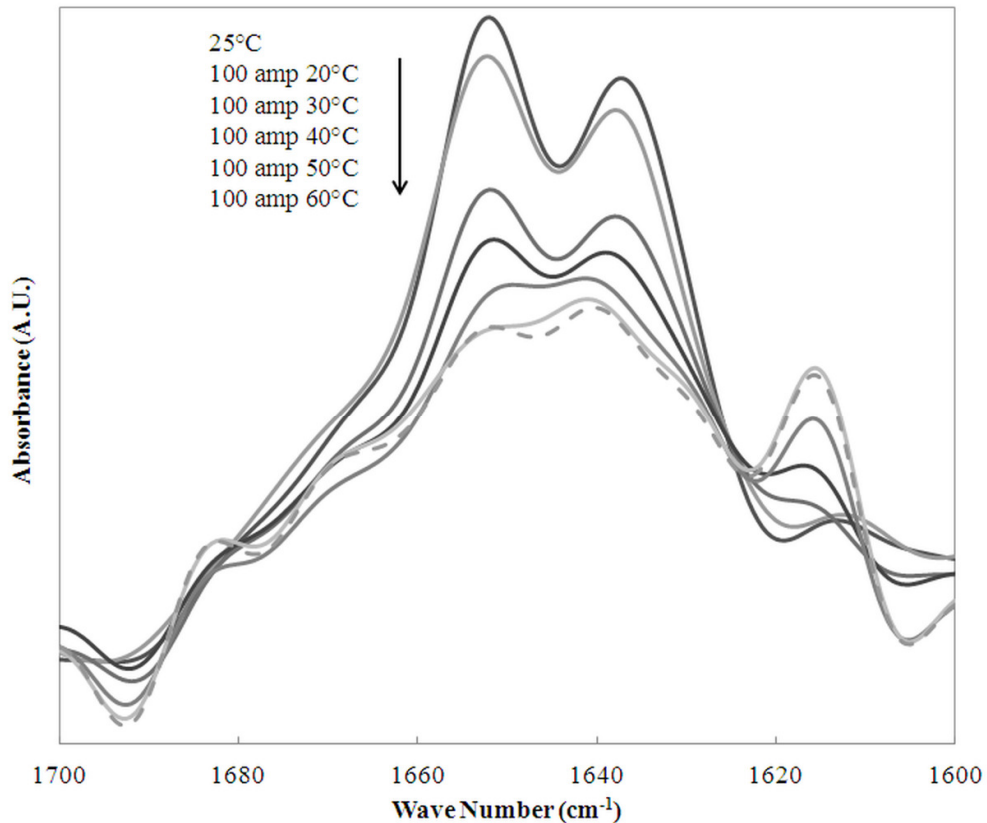
Figure 25. Representative Fourier self-deconvolution spectra of PPO in D_2O buffer recorded at different temperatures during ultrasound treatment (solid lines) and spectrum of the PPO measured at 25 ℃ after cooling from 100% amplitude 60 ℃ (dotted line).

For more precise estimation of inactivation mechanism during TS treatment, the intensities of the amide I band and its components were plotted as a function of temperature of TS treatments (Figure 26). No significant change in terms of band intensities was observed between the bands at 25 ℃ and 100% amplitude 20 ℃. As shown in graph, the intensities of the 1652 and 1635 cm^{-1} band decreased as the temperature increased during TS treatments after 100% amplitude 20 ℃ ultrasound treatment. Simultaneously, the intensity of the aggregation band at 1616 cm^{-1} increased with the increasing temperature for TS treatments. The intensity of the band increased slowly up to 100% amplitude 40 ℃ and further increase in the intensity was observed after this inactivation.
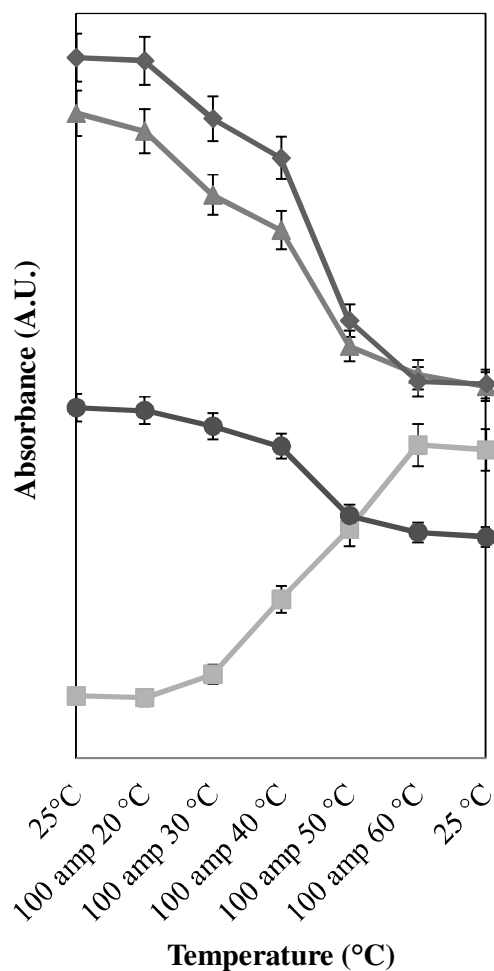
Figure 26. A plot of the changes in the intensity of the amide I and its components for PPO during TS treatment (($\blacklozenge$) 1652 cm^{-1}, ($\blacksquare$) 1616 cm^{-1}, ($\blacktriangle$) 1635 cm^{-1}, and ($\bullet$) amide I).

Using the intensity profiles, transition temperature (T_m) for the different amide I components was determined and represented in Table 6. The T_m values for α-helix, β-sheet, aggregated β-sheet structure and amide I band were determined as around 44 ºC. These values were lower than that found for thermal inactivation as about 55 ºC. This indicated that ultrasound treatment began to disrupt secondary structures of the enzyme at lower temperatures compared to the thermal inactivation. This may be associated with the different enzyme inactivation mechanism of ultrasound caused by cavitation, localized heating and free radical formation.

Table 6. Transition Temperatures (Tm) for different amide I components for PPO during TS treatment.

Structure	Amide I band (cm^{-1})	T$_m$ value (ºC)
α-helix	1652	43.86
β-sheet	1635	41.74
Aggregated β-sheet	1616	43.78
Amide I	1653	43.70

3.2.6. Curve-fitting analysis of PPO during TS Treatment

For quantitative determination of secondary structural changes during TS treatment in D$_2$O curve-fitting analysis was applied to the Amide I region (1700 – 1600 cm^{-1}). The contribution of each component band to the amide I band is shown in Figure 27 for 25 ºC and 100% amplitude 60 ºC ultrasound treatment. The bands at 1652 cm^{-1} due to the α-helix and that at 1635 cm^{-1} due to the β-sheet structure became weaker by the ultrasound treatment, whereas other bands due to the aggregated β-sheet (1683 and 1616 cm^{-1}), turns (1670 cm^{-1}) and random coil (1640 cm^{-1}) structures became stronger after 100% amplitude 60 ºC ultrasound treatment.
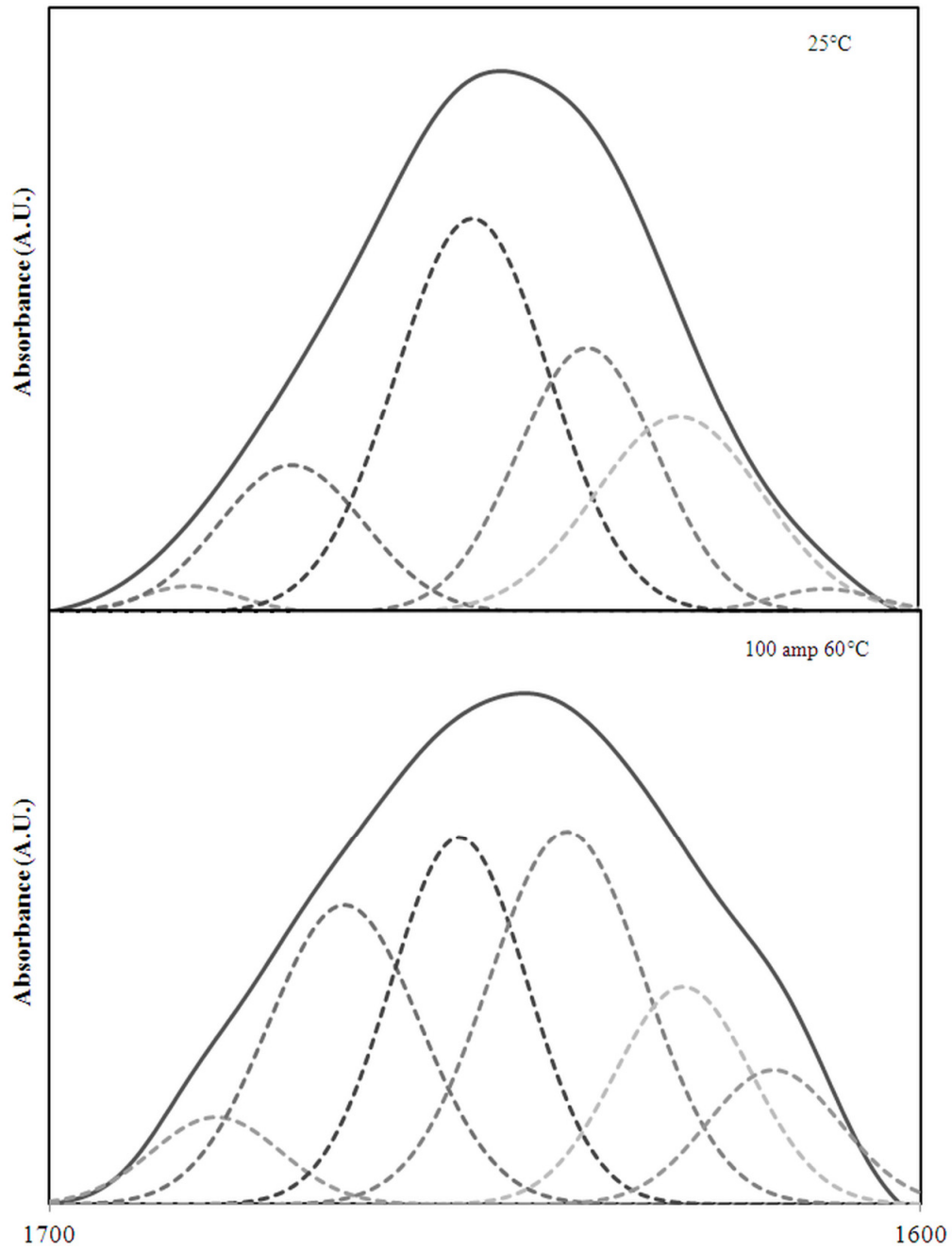
Figure 27. Curve-fitting analysis of amide I band (1700 – 1600 cm^{-1}) of PPO during TS treatment.

Secondary structural change (%) of PPO during TS treatment estimated by curve-fitting analysis is shown in Table 7. According to the curve-fitting analysis, PPO contained 38.87 ± 0.02 % α-helix, 27.91 ± 0.02 % β-sheet, 14.93 ± 0.01 % β-turn, 15.01 ± 0.01 % random coil and 3.27 ± 0.06 % aggregated β-sheet structures at 25 ºC before TS treatment. After TS treatment α-helix content decreased from 38.87 ± 0.02 % to 22.12 ± 0.26 % ($p < 0.05$), β-sheet content decreased from 27.91 ± 0.02 % to 13.42 ± 0.02 % ($p < 0.05$) whereas β-turn, random coil and aggregated β-sheet structures increased up to 23.09 ± 0.13, 26.42 ± 0.26 and 14.94 ± 0.11 %, respectively ($p < 0.05$).

Table 7. Secondary structure change (%) of PPO estimated by curve-fitting during TS treatment.

TS Temperature at 100% amplitude (ºC)	α-helix	β-sheet	β-turn	Random coil	Aggregated β-sheets
25	38.87 ± 0.02	27.91 ± 0.02	14.93 ± 0.01	15.01 ± 0.01	3.27 ± 0.06
20	36.00 ± 0.40	24.75 ± 0.98	16.18 ± 0.33	17.95 ± 0.20	5.12 ± 0.06
30	31.67 ± 0.03	21.31 ± 0.02	18.88 ± 0.25	21.18 ± 0.13	6.97 ± 0.08
40	27.39 ± 0.72	18.75 ± 0.23	20.79 ± 0.47	23.38 ± 0.10	9.68 ± 0.08
50	23.37 ± 0.01	16.56 ± 0.01	21.39 ± 0.30	25.65 ± 0.38	13.03 ± 0.10
60	22.74 ± 0.10	13.65 ± 0.04	22.79 ± 0.21	26.50 ± 0.23	14.32 ± 0.12
25 (after cooling from 60ºC)	22.12 ± 0.26	13.42 ± 0.02	23.09 ± 0.13	26.42 ± 0.26	14.94 ± 0.11

Graphical representation of the change in the secondary structure components is shown in Figure 28. This representation indicated that α-helix and β-sheet structures were lost as the temperature increase with the formation of aggregated β-sheets and the increase in the turns and disorder structure (1640 cm^{-1}).
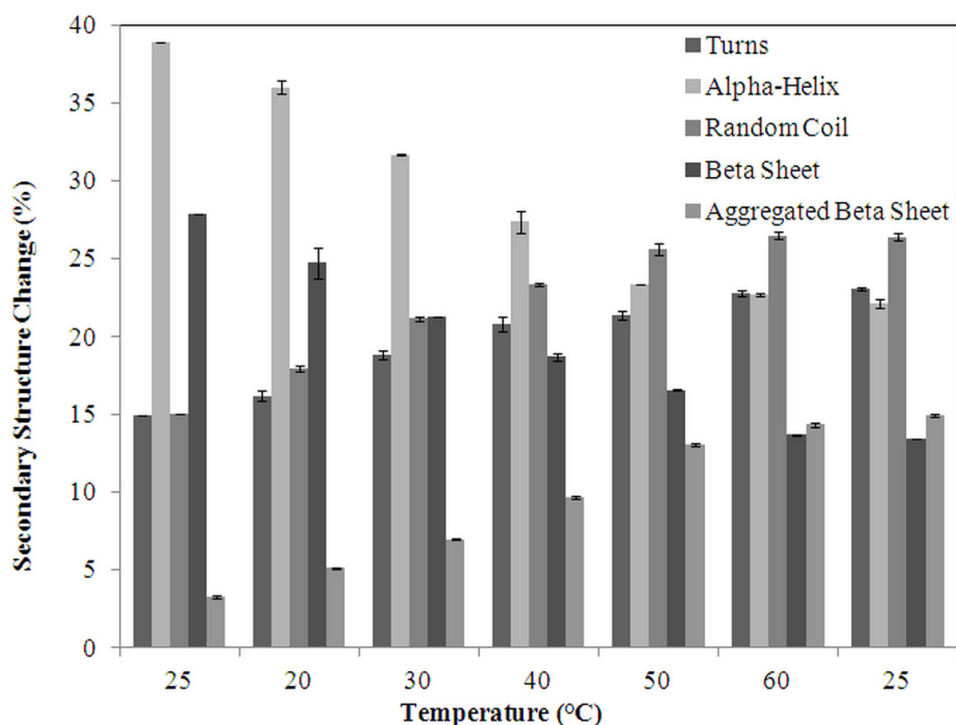
Figure 28. Graph of secondary structure change (%) of PPO according to the curve-fitting analysis during TS treatment.

FTIR studies revealed that mushroom PPO enzyme was irreversibly inactivated at 100% amplitude at 60 ℃ during thermosonication treatment whereas irreversible inactivation of the enzyme was at 70 ℃ for thermal treatment. Furthermore, T_m value of thermosonication treatment which was around 44 ℃ was lower than that of thermal treatment, which was around 55 ℃. These results suggested that thermosonication treatment began to affect the secondary structural component of the PPO enzyme at lower temperatures compared to the thermal treatment. It was also suggested from FTIR studies that conformation changes of PPO caused by ultrasound and temperature were different. At the end of the thermal treatment,

formation of aggregated β-sheet structures was higher than that found for thermosonication treatment due to the lower inactivation temperature. Heat and ultrasound combination behaved synergistically on the conformation changes of enzyme.

CHAPTER 4

CONCLUSION AND RECOMMENDATIONS

In the present study, changes in structure and activity of the PPO during thermal and thermosonication treatment were investigated. According to the inactivation studies, the enzyme activity decreased with increasing temperature and time and PPO was completely inactivated at 70°C for 5 min during thermal treatment. Similarly, as temperature, ultrasonic power and time increased, higher inactivation rate was obtained during thermosonication treatment. D value for thermal treatment at 60°C was found as 6.66 min. For 100, 80 and 60 % amplitude ultrasound treatment at same temperature D values were found as 2.09, 3.33 and 3.44 min, respectively. It was concluded from the inactivation studies that heat-ultrasound combination is seen to be more effective compared to heat treatment alone in reducing enzyme activity.

FTIR studies for thermal treatment suggested that the FTIR spectrum at 70 °C and that at 25 °C after cooling were very similar to each other. This revealed that PPO was irreversibly inactivated above 70°C compatible with the inactivation studies. It was found from the Fourier self-deconvolution analysis that the intensity of α-helix and β-sheet structure decreased when the temperature increased. However, the intensity of the aggregation bands 1616 and 1683 cm^{-1} increased with the increasing temperature and these bands still observed after inactivation at 70°C, indicating the loss of secondary structure of PPO. According to the NN analysis, it was found that PPO enzyme was α-helix dominating enzyme and contained 42.33 ± 3.06 % α-helix structure, 21.33 ± 4.73 % β-sheet structure, 19.67 ± 1.15 % turns and 16.67 ± 1.53 % random coil structure. Furthermore, similar results found for curve-fitting analysis, shown that PPO contained 38.87 ± 0.02 % α-helix, 27.91 ± 0.02 % β-sheet, 14.93 ± 0.01 % β-turn, 15.01 ± 0.01 % random coil and 3.27 ± 0.06 % aggregated β-sheet

structures. According to the curve-fitting analysis α-helix content decreased from 38.87 ± 0.02 % to 19.40 ± 0.21 % ($P < 0.05$), β-sheet content decreased from 27.91 ± 0.02 % to 15.88 ± 0.02 % ($P < 0.05$) whereas β-turn, random coil and aggregated β-sheet structures increased up to 21.93 ± 0.14, 22.47 ± 0.60 and 20.31 ± 0.27 %, respectively ($P < 0.05$).

For TS treatment, PPO was irreversibly inactivated at 100% amplitude at 60°C for 10 min according to the conformation studies. It was reported from the Fourier self-deconvolution analysis that the intensities of α-helix and β-sheet structure decreased while the temperature increased up to 60°C during TS treatment. Furthermore, the bands at 1640 cm^{-1} due to random coil and at 1670 cm^{-1} due to turns became apparent at 100% amplitude 60°C, demonstrating increase in unordered structures. According to the curve-fitting analysis, it was found that after TS treatment α-helix content decreased from 38.87 ± 0.02 % to 22.12 ± 0.26 % ($P < 0.05$), β-sheet content decreased from 27.91 ± 0.02 % to 13.42 ± 0.02 % ($P < 0.05$) whereas β-turn, random coil and aggregated β-sheet structures increased up to 23.09 ± 0.13, 26.42 ± 0.26 and 14.94 ± 0.11 %, respectively ($P < 0.05$).

In conclusion, the results gathered in this study showed that inactivation and conformation studies were consistent. Inactivation studies revealed that TS treatment was found to be more effective than thermal treatment in terms of enzyme inactivation at lower temperatures. FTIR studies showed that thermal and TS inactivation of the enzyme was not due to a small change in the active site, this was due to the global conformation change of the enzyme. It was indicated that conformation changes of PPO caused by ultrasound and heat were different. At the end of the thermal treatment formation of aggregated β-sheet structures was higher than that found for thermosonication treatment due to the higher inactivation temperature. Heat and ultrasound combination behaved synergistically with respect to the enzyme inactivation and conformation changes. The overall results suggested that mushroom PPO enzyme was inactivated at lower temperatures during thermosonication treatment compared to the thermal treatment.

As a recommendation, the research may be continued by covering with more ultrasound combinations. Manothermosonication (MTS) treatment may be studied as more effective method on the enzyme inactivation. Pulse effect of ultrasound treatment on the enzyme may be investigated. For future studies, TS treatment may be developed as an alternative food pasteurization method for the production of fruit juices such as apricots, peaches, cherries which are widely consumed in Turkey, because of its advantages. It is considered that the system established in this study will be a model for other scientific studies and create a new working area for many researchers. Furthermore, the results gathered in this study will support the usage of the ultrasound in the food industry for enzyme inactivation purposes.

REFERENCES

Abid M., Jabbar S., Hu B., Hashim M.M., Wu T., Lei S., Khan M.K., and Zeng X. (2014). Thermosonication as a potential quality enhancement technique of apple juice. *Ultrasonics Sonochemistry*, 21: 984–990.

Anese M., and Sovrano S. (2006). Kinetics of thermal inactivation of tomato lipoxygenase. *Food Chemistry*, 95: 131–137.

Anthon G.E. and Barrett D.M. (2002). Kinetic Parameters for the Thermal Inactivation of Quality-Related Enzymes in Carrots and Potatoes. *J. Agric. Food Chem.*, 50: 4119-4125.

Anthon G.E., Sekine Y.,Watanabe Y., and Barrett D.M. (2002). Thermal Inactivation of Pectin Methylesterase, Polygalacturonase, and Peroxidase in Tomato Juice. *J. Agric. Food Chem.*, 50: 6153-6159.

Barth A. (2007). Infrared spectroscopy of proteins. *Biochimica et Biophysica Acta*, 1767: 1073–1101.

Bayındırlı A., Alpas H., Bozoglu F., and Hizal M. (2006). Efficiency of high pressure treatment on inactivation of pathogenic microorganisms and enzymes in apple, orange, apricot and sour cherry juices. *Food Control*, 17; 52–58.

Carbonaro M ., and Nucara A. (2010). Secondary structure of food proteins by Fourier transform spectroscopy in the mid-infrared region. *Amino Acids*, 38: 679–690.

Cheng X.-f., Zhang M., and Adhikari B. (2013). The inactivation kinetics of polyphenol oxidase in mushroom (*Agaricus bisporus*) during thermal and thermosonic treatments. *Ultrasonics Sonochemistry*, 20: 674–679.

Chutintrasri, B.; Noomhorm, A. (2006). Thermal inactivation of polyphenoloxidase in pineapple puree. *LWT – Food Sci. Technol.*, 3: 492–495.

Cruz R.M.S., Vieira M.C., and Silva C.L.M. (2006). Effect of heat and thermosonication treatments on peroxidase inactivation kinetics in watercress (Nasturtium officinale). *Journal of Food Engineering*, 72: 8–15.

Dalmadi, I.; Rapeanu, G.; Van Loey, A.; Smout, C.; Hendrickx, M. (2006). Characterization and inactivation by thermal and pressure processing of strawberry (*Fragaria ananassa*) polyphenol oxidase: a kinetic study. *J. Food Biochem.*, 30: 56–76.

Damodaran, S. (2008). Amino Acids, Peptides, and Proteins. In S. Damodaran, K.L. Parkin, and O.R Fennema, *Fennema's Food Chemistry Fourth Edition* (pp.217-329). Boca Raton: CRC Press.

De Gennaro, L., Cavella, S., Romano, R., & Masi, P. (1999). The use of ultrasound in food technology I: inactivation of peroxidase by thermosonication. *Journal of Food Engineering*, 39: 401–407.

Demirdöven and Baysal T. (2009). The Use of Ultrasound and Combined Technologies in Food Preservation. *Food Reviews International*, 25: 1–11.

Dirix C., Duvetter T., Loey A.V., Hendrickx M. and Heremans K. (2005). The in situ observation of the temperature and pressure stability of recombinant Aspergillus aculeatus pectin methylesterase with Fourier transform IR spectroscopy reveals an unusual pressure stability of β-helices. *Biochem. J.*, 392: 565–571.

Fellows, P.J. (2000). *Food Processing Technology: Principles & Practice*, Boca Raton: CRC Press LLC.

Garip S. and Severcan F. (2010). Determination of simvastatin-induced changes in bone composition and structure by Fourier transform infrared spectroscopy in rat animal model. *Journal of Pharmaceutical and Biomedical Analysis*, 52: 580–588.

Garip S., Yapici E., Simsek Ozek N., Severcan M. and Severcan F. (2010). Evaluation and discrimination of simvastatin-induced structural alterations in proteins of different rat tissues by FTIR spectroscopy and neural network analysis. *Analyst*, 135: 3233–3241.

Gouzi, H., Depagne, C., and Coradin, T. (2012). Kinetics and Thermodynamics of the Thermal Inactivation of Polyphenol Oxidase in an Aqueous Extract from *Agaricus bisporus*. J. Agric.Food Chem.; 60, 500−506.

Gökmen V., Bahçeci K.S., Serpen A., and Acar J. (2005). Study of lipoxygenase and peroxidase as blanching indicator enzymes in peas: change of enzyme activity, ascorbic acid and chlorophylls during frozen storage. *LWT*, 38: 903–908.

Grandison A.S. (2006). Postharvest Handling and Preparation of Foods for Processing. In J.G. Brennan. *Food Processing Handbook* (pp. 1-31). Weinheim, Germany, Wiley-VCH.

Greenfield N.J. (2006). Using circular dichroism spectra to estimate protein secondary structure. *Nat Protoc.*, 1(6): 2876–2890.

Gülseren I., Güzey D., Bruce B.D., and Weiss J. (2007). Structural and functional changes in ultrasonicated bovine serum albumin solutions. *Ultrasonics Sonochemistry*, 14: 173–183.

Güneş, B. and Bayındırlı, A. (1993). Peroxidase and Lipoxygenase Inactivation During Blanching of Green Beans, Green Peas and Carrots. *Lebensmittel Wissenschaft und Technologie - Food Science and Technology*, 26: 406-410.

Haris P.I., and Severcan F. (1999). FTIR spectroscopic characterization of protein structure in aqueous and non-aqueous media. *Journal of Molecular Catalysis B: Enzymatic*, 7: 207–221.

Hendrickx M., Ludikhuyze L., Van den Broeck I. and Weemaes C. (1998). Effects of High Pressure on Enzymes Related to Food Quality. *Trends in Food Science & Technology*, 9: 197-203.

Ionita E., Aprodu I., Stanciuc N., Rapeanu G., and Bahrim G.. (2014). Advances in structure–function relationships of tyrosinase from *Agaricus bisporus* – Investigation on heat-induced conformational Changes. *Food Chemistry*, 156: 129–136.

Ismaya W.T., Rozeboom H.J., Weijn A., Mes J.J., Fusetti F., Wichers H.J., and Dijkstra B.W. (2011). Crystal Structure of *Agaricus bisporus* Mushroom Tyrosinase: Identity of the Tetramer Subunits and Interaction with Tropolone. *Biochemistry,* 50: 5477–5486.

Kadkhodaee R. and Povey MJW. (2008). Ultrasonic inactivation of Bacillus a-amylase. I. Effect of gas content and emitting face of probe. *Ultrasonics Sonochem*, 15 (2): 133-142.

Karoui R., Pierna J.A.F. and Dufour E. (2008). Mid-infrared (MIR) and Fourier Transform Mid-infrared (FT-MIR) Spectroscopies. In: D.-W. Sun, *Modern Techniques for Food Authentication* (pp. 27-64). Academic Press.

Kuldiloke J., Eshtiaghi M., Zenker M., and Knorr D. (2007). Inactivation of Lemon Pectinesterase by Thermosonication. *International Journal of Food Engineering*, 3(2): Art. 3.

Lewis M.J., and Heppell N.J. (2000). *Continuous thermal processing of foods: pasteurization and UHT sterilization*, Aspen Publishers, Inc.

Leadley C.E., and Williams A. (2006). Pulsed Electric Field Processing, Power Ultrasound and Other Emerging Technologies. In J.G. Brennan. *Food Processing Handbook* (pp. 201-235). Weinheim, Germany, Wiley-VCH.

Liu W., Liu J., Liu C., Zhong Y., Liu W., and Wan J. (2009). Activation and conformational changes of mushroom polyphenoloxidase by high pressure microfluidization treatment. *Innovative Food Science and Emerging Technologies*, 10: 142–147.

Liu B, Ma HL, Li SJ, Zhao WR, and Li L. (2010). Study on the effect of ultrasound on the secondary structure of BSA by FTIR. *Guang Pu Xue Yu Guang Pu Fen Xi*, 30(8): 2072-6.

Liu W., Zou L., Liu J., Zhang Z., Liu C., and Liang R. (2013). The effect of citric acid on the activity, thermodynamics and conformation of mushroom polyphenoloxidase. *Food Chemistry*, 140: 289–295.

Lopez, P., Sala, F. J., Fuente, J. L., Condon, S., Raso, J., and Burgos, J. (1994). Inactivation of peroxidase, lipoxygenase and polyphenol oxidase by manothermosonication. *Journal of Agricultural and Food Chemistry*, 42(2): 253–256.

Lopez P. and Burgos J. (1995). Lipoxygenase Inactivation by Manothermosonication: Effects of Sonication Physical Parameters, pH, KCl, Sugars, Glycerol, and Enzyme Concentration. *J. Agric. Food Chem.*, 43: 620-625.

Ludikhuyze L., Van Loey A., Smout I.C., Hendrickx M. (2003). Effects of Combined Pressure and Temperature on Enzymes Related to Quality of Fruits and Vegetables: From Kinetic Information to Process Engineering Aspects. *Critical Reviews in Food Science and Nutrition*, 43(5): 527–586.

Manas P., Munoz B., Sanz D., and Condon S. (2006). Inactivation of lysozyme by ultrasonic waves under pressure at different temperatures. *Enzyme and Microbial Technology*, 39: 1177–1182.

Mantsch H.H. (2001). Historical Survey of Infrared and Raman Spectroscopy of Biological Materials. In H.U. Gremlich and B. Yan. *Infrared and Raman Spectroscopy of Biological Materials* (pp. 1-14). Marcel Dekker, Inc.

Marchioni C., Riccardi E., Spinelli S., Dell'Unto F., Grimaldi P., Bedini A., Giliberti C., Giuliani L., Palomba R., and Congiu Castellano A. (2009). Structural changes induced in proteins by therapeutic ultrasounds. *Ultrasonics*, 49: 569–576.

Mason, H.S. (1956).Structures and functions of the phenolase complex. *Nature*, 177: 79–81.

Mawson R., Gamage M., Terefe N.S., and Knoerzer K. (2010). Ultrasound in enzyme activation and inactivation. In: H. Feng, G. Barbosa-Canovas, J. Weiss, *Ultrasound technologies for food and bioprocessing* (pp. 369–404), New York, Springer.

Mayer, A.M., and Harel, E. (1979). Polyphenol oxidases in plants. *Phytochemistry*, 18: 193–215.

McCord, J.D. and Kilara, A. (1983). Control of enzymatic browning in processed mushrooms (*Agaricus bisporus*). *J. Food Sci.*, 48: 1479-1483.

Morales-Blancas E.F., Chandia V.E., and Cisneros-Zevallos L. (2002). Thermal Inactivation Kinetics of Peroxidase and Lipoxygenase from Broccoli, Green Asparagus and Carrots. *Journal of Food Science*, 67(1).

Murayama K. and Tomida M. (2004). Heat-Induced Secondary Structure and Conformation Change of Bovine Serum Albumin Investigated by Fourier Transform Infrared Spectroscopy. *Biochemistry*, 43: 11526-11532.

Mustapha K., and Ghalem S-A. (2007). Effect of heat treatment on polyphenol oxidase and peroxidase activities in Algerian stored dates. *African Journal of Biotechnology*, 6(6): 790-794.

Ndiaye C., Xu S-H., Wang Z. (2009). Steam blanching effect on polyphenoloxidase, peroxidase and colour of mango (Mangifera indica L.) slices. *Food Chemistry*, 113: 92-95.

Nelson D.L. and Cox M.M. (2008). *Lehninger Principles of Biochemistry Fifth Edition*. New York : W.H. Freeman.

O'Donnell C.P., Tiwari B.K., Bourke P. and Cullen P.J. (2010). Effect of ultrasonic processing on food enzymes of industrial importance. *Trends in Food Science & Technology*, 21: 358-367.

Oey I. (2010). Effect of Novel Food Processing on Fruit and Vegetable Enzymes. In A. Bayındırlı, *Enzymes in Fruit and Vegetable Processing: Chemistry and Engineering Applications* (pp: 245-313). New York: CRC Press.

Parkin, K.L. (2008). Enzymes. In S. Damodaran, K.L. Parkin, and O.R Fennema, *Fennema's Food Chemistry Fourth Edition* (pp.217-329). Boca Raton: CRC Press.

Platis D., Kotzia G.A., Axarli I.A., and Labrou N.E. (2006). Enzyme Engineering and Technology. In Y.H. Hui, *Food Biochemistry and Food Processing*. Blackwell Publishing.

Queiroz C., Mendes Lopes M.L., Fialho E., and Valente-Mesquita V.L. (2008). Polyphenol Oxidase: Characteristics and Mechanisms of Browning Control. *Food Reviews International*, 24: 361-375.

Ramesh M.N. (2007). Pasteurization and Food Preservation. In M.S. Rahman, *Handbook of Food Preservation Second Edition* (pp.571-583). Boca Raton: CRC Press.

Rapeanu, G.; Loey, A.V.; Smout, C.; Hendrickx, M. (2006). Biochemical characterization and process stability of polyphenoloxidase extracted from Victoria grape (*Vitis vinifera* ssp. *Sativa*). *Food Chem.*, 94: 253-361.

Sala F.J., Burgos J., Condon S., Lopez P., and Raso J. (1995). Effect of heat and ultrasound on microorganisms and enzymes. In G.W. Gould, *New Methods of Food Preservation* (pp. 176-204). Glasgow, Blackie Academic and Professional.

Savadkoohi S., Bannikova A, Kasapis S., and Adhikari B. (2014). Structural behaviour in condensed bovine serum albumin systems following application of high pressure. *Food Chemistry*, 150: 469-476.

Schweiggert U., Schieber A., and Carle R. (2005). Inactivation of peroxidase, polyphenoloxidase, and lipoxygenase in paprika and chili powder after immediate thermal treatment of the plant material. *Innovative Food Science and Emerging Technologies*, 6: 403 - 411.

Severcan M., Severcan F., and Haris P.I. (2001). Estimation of protein secondary structure from FTIR spectra using neural networks. *Journal of Molecular Structure*, 565-566: 383-387.

Severcan F. and Haris P. (2003). Fourier Transform Infrared Spectroscopy Suggests Unfolding of Loop Structures Precedes Complete Unfolding of Pig Citrate Synthase. *Biopolymers*, 69: 440-447.

Shi C., Dai Y., Liu Q., Xie Y, and Xu X. (2003). The FT-IR spectrometric analysis of the changes of polyphenol oxidase II secondary structure. *Journal of Molecular Structure*, 644: 139-144.

Smeller L., Meersman,F., Fidy J. and Heremans K. (2003). High-Pressure FTIR Study of the Stability of Horseradish Peroxidase. Effect of Heme Substitution, Ligand Binding, Ca^{++} Removal, and Reduction of the Disulfide Bonds. *Biochemistry*, 42: 553-561.

Stuart B. and Ando D.J. (1997). *Biological Applications of Infrared Spectroscopy*. John Wiley and Sons.

Stuart B. (2004). *Infrared Spectroscopy: Fundamentals and Applications*. John Wiley and Sons.

Sun N.K. and Song K.B. (2003). Effect of Nonthermal Treatment on the Molecular Properties of Mushroom Polyphenoloxidase. *Journal of Food Science*, 68(5): 1639-1643.

Şimşek Ş., and Yemenicioğlu A. (2007). Partial purification and kinetic characterization of mushroom stem polyphenoloxidase and determination of its storage stability in different lyophilized forms. *Process Biochemistry*, 42: 943-950.

Thakur B.R. and Nelson P.E. (1997). Inactivation of lipoxygenase in whole soy flour suspension by ultrasonic cavitation. *Nahrung*, 41(5): 299-301.

Tijskens L.M.M., Rodis P.S., Hertog M. L. A. T. M., Waldron K.W., Ingham L., Proxenia N. and Van Dijk C. (1997). Activity of Peroxidase during Blanching of Peaches, Carrots and Potatoes. *Journal of Food Engineering*, 34: 355-370.

Tolbert, N.E. (1973). Activation of polyphenol oxidase of chloroplasts. *Plant. Physiol.*, 51: 234-244.

Tomas-Barberan, F.A. and Espin J.C. (2001). Phenolic compounds and related enzymes as determinants of quality in fruits and vegetables. *J. Sci. Food Agric.*, 81: 853-876.

Torley P.J., and Bhandari B.R. (2007). Ultrasound in Food Processing and Preservation. In M.S. Rahman, *Handbook of Food Preservation Second Edition* (pp.571-583). Boca Raton: CRC Press.

Tse M., Kermasha S., and Ismail A. (1997). Biocatalysis by tyrosinase in organic solvent media; a model system using catechin and vanillin as substrates. *Journal of Molecular Catalysis B: Enzymatic*, 2: 199-213.

Tsou, C.-L. (1986). Location of the Active Sites of Some Enzymes in Limited and Flexible Molecular Regions. *Trends Biochem. Sci.*, 11: 427-429.

Underkofler L.A. (1980). Enzymes. In T.E.Furia, *CRC Handbook of Food Additives* (pp.57-125). CRC Press.

Vamos-Vigyazo, L. (1981). Polyphenol oxidase and peroxidase in fruits and vegetables. *Crit. Rev. Food Sci. Nutr.*, 15: 49-127.

Versteeg, C.; Rombouts, F. M.; Spaansen, C. H.; Pilnik, W. (1980). Thermostability and orange juice cloud stabilizing properties of multiple pectinesterases from orange. *J. Food Sci.*, 45: 969-971, 998.

Weemaes C., Rubens P., De Cordt S., Ludikhuyze L., Van Den Broeck I., Hendrickx M., Heremans K., and Tobback P. (1997). Temperature Sensitivity and Pressure Resistance of Mushroom Polyphenoloxidase. *Journal of Food Science,* 62(2): 261 - 266.

Whitaker, J.R. (1994). *Principles of Enzymology for the Food Sciences.* Marcel Dekker, INC.

Wu J.-J., Cheng K.-W., Li E.T.S., Wang M., and Ye W.-C. (2008). Antibrowning Activity of MRPs in Enzyme and Fresh-Cut Apple Slice Models. *Food Chemistry*, 109: 379-385.

Yemenicioğlu A., Özkan M., and Cemeroğlu B. (1997). Heat Inactivation Kinetics of Apple Polyphenoloxidase and Activation of its Latent Form. *Journal of Food Science*, 62(3).

Yi J.Y., Dong P., Wang Y.T., Jiang B., Liao X.J., Hu X.S., Zhang Y. (2012). Study on the Effect of High Hydrostatic Pressure Treatment on the Secondary Structure of Mushroom Polyphenoloxidase by SRCD and FTIR. *Guang Pu Xue Yu Guang Pu Fen Xi/Spectroscopy and Spectral Analysis*, 32(2): 317-323.

Yu Z-L., Zeng W-C., Zhang W-H., Liao X-P., Shi B. (2014). Effect of ultrasound on the activity and conformation of α-amylase, papain and pepsin. *Ultrasonics Sonochemistry*, 21: 930-936.

ANOVA TABLES

Table A. 1. ANOVA table for thermal inactivation of mushroom PPO.

% Residual versus Time, Temp

Factor Type Levels Values

Time   fixed   7   0, 5, 10, 15, 20, 25, 30

Temp   fixed   6   20, 30, 40, 50, 60, 70

Analysis of Variance for % Residual Activity, using Adjusted SS for Tests

Source	DF	Seq SS	Adj SS	Adj MS	F	P
Time	6	4860.9	4860.9	810.1	504.74	0.000
Temp	5	224206.0	224206.0	44841.2	27937.13	0.000
Time*Temp	30	6749.7	6749.7	225.0	140.17	0.000
Error	84	134.8	134.8	1.6		
Total	125	235951.5				

$S = 1.26692$ R-Sq = 99.94%   R-Sq (adj) = 99.91%

Grouping Information Using Tukey Method and 95.0% Confidence

Time	N	Mean	Grouping				
0	18	71.1	A				
5	18	63.4		B			
10	18	57.1			C		
15	18	55.8			C		
20	18	54.4				D	
25	18	52.9					E
30	18	52.3					E

Means that do not share a letter are significantly different.

Grouping Information Using Tukey Method and 95.0% Confidence

Temp	N	Mean	Grouping				
30	21	100	A				
20	21	100	A				
40	21	95		B			
50	21	43			C		
60	21	10.3				D	
70	21	1.1					E

Means that do not share a letter are significantly different.

Table A. 2. ANOVA table for thermosonic inactivation of mushroom PPO

Residual Activity versus Time, Temp, Amplitude

Factor	Type	Levels	Values
Time	fixed	7	0, 5, 10, 15, 20, 25, 30
Temp	fixed	5	20, 30, 40, 50, 60
Amplitude	fixed	3	60, 80, 100

Analysis of Variance for % Residual Activity, using Adjusted SS for Tests

Source	DF	Seq SS	Adj SS	Adj MS	F	P
Time	6	47074.6	46590.8	7765.1	5179.21	0.000
Temp	4	330441.3	330793.1	82698.3	55158.42	0.000
Amplitude	2	1509.8	1570.4	785.2	523.73	0.000
Time*Temp	24	14074.3	13983.9	582.7	388.63	0.000
Time*Amplitude	12	1005.9	1001.9	83.5	55.69	0.000
Temp*Amplitude	8	341.1	341.7	42.7	28.49	0.000
Time*Temp*Amplitude	48	1519.6	1519.6	31.7	21.12	0.000
Error	210	314.9	314.9	1.5		
Total	314	396281.4				

S = 1.22445   R-Sq = 99.92%   R-Sq (adj) = 99.88%

Grouping Information Using Tukey Method and 95.0% Confidence

Time	N	Mean	Grouping						
0	45	83.9	A						
5	45	64.7		B					
10	45	58.3			C				
15	45	55.0				D			
20	45	51.0					E		
25	45	48.7						F	
30	45	45.0							G

Means that do not share a letter are significantly different.

Grouping Information Using Tukey Method and 95.0% Confidence

Temp	N	Mean	Grouping				
20	63	92.1	A				
30	64	85.7		B			
40	62	73.5			C		
50	63	30.6				D	
60	63	8.6					E

Means that do not share a letter are significantly different.

Grouping Information Using Tukey Method and 95.0% Confidence

Amplitude	N	Mean	Grouping		
60	105	60.4	A		
80	105	58.2		B	
100	105	55.7			C

Means that do not share a letter are significantly different.

Table A. 3. ANOVA tables for intensity changes during TS treatment.

Intensity change of 1651 cm^{-1} versus TS Temperature

Factor Type Levels Values

Temperature fixed 7 25, 20, 30, 40, 50, 60, 25

Analysis of Variance for intensity change of 1651 cm^{-1}, using Adjusted SS for Tests

Source	DF	Seq SS	Adj SS	Adj MS	F	P
Temperature	6	0.340628	0.340628	0.056771	64.27	0.000
Error	14	0.012367	0.012367	0.000883		
Total	20	0.352996				

S = 0.02972 R-Sq = 96.50% R-Sq (adj) = 94.99%

Grouping Information Using Tukey Method

Temperature	N	Mean	Grouping
25	3	0.75867	A
20	3	0.75567	A
30	3	0.70133	A B
40	3	0.66433	B
50	3	0.51133	C
60	3	0.45400	C
25(cooling from 70)	3	0.45200	C

Means that do not share a letter are significantly different.

Intensity change of 1615 cm^{-1} versus TS Temperature

Factor   Type   Levels   Values
Temperature   fixed   7   25, 20, 30, 40, 50, 60, 25

Analysis of Variance for intensity change of 1615 cm^{-1}, using Adjusted SS for Tests

Source	DF	Seq SS	Adj SS	Adj MS	F	P
Temperature	6	0.196782	0. 196782	0.032797	222.34	0.000
Error	14	0.002065	0.002065	0.000148		
Total	20	0.198848				

S = 0.01215   R-Sq = 98.96%   R-Sq (adj) = 98.52%

Grouping Information Using Tukey Method

Temperature	N	Mean	Grouping			
60	3	0.39450	A			
25(cooling from 70)	3	0.39000	A			
50	3	0.31533		B		
40	3	0.24933			C	
30	3	0.17900				D
25	3	0.15867				D
20	3	0.15667				D

Means that do not share a letter are significantly different.

Intensity change of 1638 cm^{-1} versus TS Temperature

Factor   Type   Levels   Values
Temperature   fixed   7   25, 20, 30, 40, 50, 60, 25

Analysis of Variance for intensity change of 1638 cm^{-1}, using Adjusted SS for Tests

Source	DF	Seq SS	Adj SS	Adj MS	F	P
Temperature	6	0.209273	0.209273	0.034879	81.81	0.000
Error	14	0.005969	0.005969	0.000426		
Total	20	0.215241				

S = 0.02065   R-Sq = 97.23%   R-Sq (adj) = 96.04%

Grouping Information Using Tukey Method

Temperature	N	Mean	Grouping
25	3	0.70633	A
20	3	0.68967	A
30	3	0.62967	B
40	3	0.56593	C
50	3	0.48757	D
60	3	0.46070	D
25(cooling from 70)	3	0.44945	D

Means that do not share a letter are significantly different.

Intensity change of Amide I versus TS Temperature

Factor   Type   Levels   Values
Temperature fixed   7   25, 20, 30, 40, 50, 60, 25

Analysis of Variance for intensity change of Amide I, using Adjusted SS for Tests

Source	DF	Seq SS	Adj SS	Adj MS	F	P
Temperature	6	0.053904	0.053904	0.008984	61.08	0.000
Error	14	0.002059	0.002059	0.000147		
Total	20	0.055963				

$S = 0.01213$ R-Sq = 96.32%   R-Sq (adj) = 94.74%

Grouping Information Using Tukey Method

Temperature	N	Mean	Grouping
25	3	0.42967	A
20	3	0.42700	A B
30	3	0.41233	A B
40	3	0.39333	B
50	3	0.32833	C
60	3	0.31250	C
25(cooling from 70)	3	0.30800	C

Means that do not share a letter are significantly different.

Table A. 4. ANOVA tables for curve-fitting analysis during thermal treatment.

% change of α-helix content versus Temperature

Factor   Type   Levels   Values
Temperature   fixed   7   25, 30, 40, 50, 60, 70, 25

Analysis of Variance for % change of α-helix content, using Adjusted SS for Tests

Source	DF	Seq SS	Adj SS	Adj MS	F	P
Temperature	6	1029.29	1029.29	171.55	20567.21	0.000
Error	14	0.12	0.12	0.01		
Total	20	1029.40				

S = 0.0913282   R-Sq = 99.99%   R-Sq (adj) = 99.98%

Grouping Information Using Tukey Method

Temperature	N	Mean	Grouping
25	3	38.8697	A
30	3	35.6846	B
40	3	26.9084	C
50	3	25.4160	D
60	3	24.0143	E
70	3	19.4052	F
25(cooling from 70)	3	19.4013	F

Means that do not share a letter are significantly different.

% change of β-sheet content versus Temperature

Factor   Type   Levels Values
Temperature fixed   7   25, 20, 30, 40, 50, 60, 25

Analysis of Variance for % change of β-sheet content, using Adjusted SS for Tests

Source	DF	Seq SS	Adj SS	Adj MS	F	P
Temperature	6	379.853	379.853	63.309	5460.36	0.000
Error	14	0.162	0.162	0.012		
Total	20	380.015				

S = 0.107677   R-Sq = 99.96%   R-Sq (adj) = 99.94%

Grouping Information Using Tukey Method

Temperature	N	Mean	Grouping
25	3	27.910	A
30	3	25.137	B
40	3	22.828	C
50	3	19.502	D
60	3	18.239	E
70	3	16.249	F
25(cooling from 70)	3	15.882	F

Means that do not share a letter are significantly different.

% change of β-turn content versus Temperature

Factor   Type   Levels   Values
Temperature fixed   7   25, 20, 30, 40, 50, 60, 25

Analysis of Variance for % change of β-turn content, using Adjusted SS for Tests

Source	DF	Seq SS	Adj SS	Adj MS	F	P
Temperature	6	151.635	151.635	25.273	4753.79	0.000
Error	14	0.074	0.074	0.005		
Total	20	151.709				

S = 0.0729128   R-Sq = 99.95%   R-Sq (adj) = 99.93%

Grouping Information Using Tukey Method

Temperature	N	Mean	Grouping				
25(cooling from 70)	3	21.9319	A				
70	3	21.6760		B			
40	3	18.0672			C		
60	3	17.6684				D	
50	3	16.8133					E
25	3	14.9324						F
30	3	14.7377						F

Means that do not share a letter are significantly different.

% change of random coil content versus Temperature

Factor Type Levels Values
Temperature fixed 7 25, 20, 30, 40, 50, 60, 25

Analysis of Variance for % change of random coil content, using Adjusted SS for Tests

Source	DF	Seq SS	Adj SS	Adj MS	F	P
Temperature	6	129.708	129.708	21.618	373.25	0.000
Error	14	0.811	0.811	0.058		
Total	20	130.518				

S = 0.240660 R-Sq = 99.38% R-Sq (adj) = 99.11%

Grouping Information Using Tukey Method

Temperature	N	Mean	Grouping
70	3	22.4764	A
25(cooling from 70)	3	22.4708	A
50	3	22.2231	A
40	3	21.9183	A
60	3	21.2032	B
30	3	19.9369	C
25	3	15.0147	D

Means that do not share a letter are significantly different.

% change of aggregated β-sheet content versus Temperature

Factor   Type   Levels Values
Temperature   fixed   7   25, 20, 30, 40, 50, 60, 25

Analysis of Variance for % change of aggregated β-sheet content, using Adjusted SS for Tests

Source	DF	Seq SS	Adj SS	Adj MS	F	P
Temperature	6	967.09	967.09	161.18	4770.24	0.000
Error	14	0.47	0.47	0.03		
Total	20	967.56				

S = 0.183818   R-Sq = 99.95%   R-Sq (adj) = 99.93%

Grouping Information Using Tukey Method

Temperature	N	Mean	Grouping
25(cooling from 70)	3	20.314	A
70	3	20.194	A
60	3	18.875	B
50	3	16.046	C
40	3	10.278	D
30	3	4.504	E
25	3	3.273	F

Means that do not share a letter are significantly different.

Table A. 5. ANOVA tables for curve-fitting analysis during TS treatment.

% change of α-helix content versus Temperature

Factor   Type   Levels   Values
Temperature fixed   7   25, 20, 30, 40, 50, 60, 25

Analysis of Variance for % change of α-helix content, using Adjusted SS for Tests

Source	DF	Seq SS	Adj SS	Adj MS	F	P
Temperature	6	705.30	705.30	117.55	2734.73	0.000
Error	14	0.60	0.60	0.04		
Total	20	705.90				

S = 0.207326   R-Sq = 99.91%   R-Sq (adj) = 99.88%

Grouping Information Using Tukey Method

Temperature	N	Mean	Grouping
25	3	38.870	A
20	3	36.000	B
30	3	31.666	C
40	3	27.394	D
50	3	23.367	E
60	3	22.741	F
25(cooling from 70)	3	22.125	F

Means that do not share a letter are significantly different.

% change of β-sheet content versus Temperature

Factor   Type   Levels Values
Temperature fixed   7   25, 20, 30, 40, 50, 60, 25

Analysis of Variance for % change of β-sheet content, using Adjusted SS for Tests

Source	DF	Seq SS	Adj SS	Adj MS	F	P
Temperature	6	590.307	590.307	98.384	2032.53	0.000
Error	14	0.678	0.678	0.048		
Total	20	590.984				

S = 0.220011   R-Sq = 99.89%   R-Sq (adj) = 99.84%

Grouping Information Using Tukey Method

Temperature	N	Mean	Grouping
25	3	27.910	A
20	3	24.750	B
30	3	21.306	C
40	3	18.746	D
50	3	16.560	E
60	3	13.649	F
25(cooling from 70)	3	13.423	F

Means that do not share a letter are significantly different.

% change of β-turn content versus Temperature

Factor   Type   Levels   Values
Temperature   fixed   7   25, 20, 30, 40, 50, 60, 25

Analysis of Variance for % change of β-turn content, using Adjusted SS for Tests

Source	DF	Seq SS	Adj SS	Adj MS	F	P
Temperature	6	166.815	166.815	27.802	568.78	0.000
Error	14	0.684	0.684	0.049		
Total	20	167.499				

S = 0.221091   R-Sq = 99.59%   R-Sq (adj) = 99.42%

Grouping Information Using Tukey Method

Temperature	N	Mean	Grouping
25(cooling from 70)	3	23.0936	A
60	3	22.7931	A
50	3	21.3895	B
40	3	20.7943	B
30	3	18.8783	C
20	3	16.1811	D
25	3	14.9324	E

Means that do not share a letter are significantly different.

% change of random coil content versus Temperature

Factor   Type   Levels   Values
Temperature fixed   7   25, 20, 30, 40, 50, 60, 25

Analysis of Variance for % change of random coil content, using Adjusted SS for Tests

Source	DF	Seq SS	Adj SS	Adj MS	F	P
Temperature	6	335.312	335.312	55.885	2473.88	0.000
Error	14	0.316	0.316	0.023		
Total	20	335.629				

S = 0.150300   R-Sq = 99.91%   R-Sq (adj) = 99.87%

Grouping Information Using Tukey Method

Temperature	N	Mean	Grouping
60	3	26.498	A
25(cooling from 70)	3	26.418	A
50	3	25.652	B
40	3	23.381	C
30	3	21.182	D
20	3	17.950	E
25	3	15.015	F

Means that do not share a letter are significantly different.

% change of aggregated β-sheet content versus Temperature

Factor   Type   Levels Values
Temperature fixed   7   25, 20, 30, 40, 50, 60, 25

Analysis of Variance for % change of aggregated β-sheet content, using Adjusted SS for Tests

Source	DF	Seq SS	Adj SS	Adj MS	F	P
Temperature	6	381.774	381.774	63.629	13870.97	0.000
Error	14	0.064	0.064	0.005		
Total	20	381.839				

$S = 0.0677290$ R-Sq = 99.98%   R-Sq (adj) = 99.98%

Grouping Information Using Tukey Method

Temperature	N	Mean	Grouping
25(cooling from 70)	3	14.9414	A
60	3	14.3187	B
50	3	13.0314	C
40	3	9.6848	D
30	3	6.9673	E
20	3	5.1223	F
25	3	3.2731	G

Means that do not share a letter are significantly different.

CURRICULUM VITAE

PERSONAL INFORMATION

Surname, Name: BALTACIOĞLU, Hande

Nationality: Turkish (TC)

Date and Place of Birth: 25 October 1979, Mersin

Marital Status: Married

Phone: +90 312 210 56 37

Cell Phone: +90 533 607 5401

Fax: +90 312 210 2767

e-mail: bhande@metu.edu.tr

EDUCATION

Degree	Institution	Year of Graduation
MS	Ankara University Food Engineering	2004
BS	Ankara University Food Engineering	2001
High School	Tevfik Sırrı Gür High School, Mersin	1996

WORK EXPERIENCE

Year	Place	Enrollment
2005-Present	METU Food Engineering	Teaching Assistant

FOREIGN LANGUAGES

English

PUBLICATIONS

Full paper in International Journals

Baltacıoğlu, H. and Artık N. (2013). Study of Post Harvest Changes in the Chemical Composition of Persimmon by HPLC. Turk J. Agric. Forest, 37: 568-574.

Conference Paper (International)

Full paper presented at and published in the proceedings of a conference by an international organization

Baltacıoğlu, H., Bayındırlı A. and Severcan F. Inactivation of Mushroom Polyphenoloxidase (PPO) by Thermosonication. 4th International Conference on Food Engineering and Biotechnology. 19-20 May 2013, Copenhagen, Denmark.

Abstract of a paper presented at and published in the proceedings of a by an international organization

Baltacıoğlu, H., and Artık N. Determination of Phenolic Compounds of Persimmon Fruit by HPLC. 1st International Congress on Food Technology. November 3-6, 2010, Antalya, Türkiye.

Baltacıoğlu, H., and Artık N. Changes in Total Phenolic Contents of Persimmon Fruits during Ripening. 4th International Congress on Food and Nutrition together with 3rd Consortium International Congress on Food Safety. 12 – 14 October 2011, İstanbul, Türkiye.

Baltacıoğlu, H., Bayındırlı A. and Severcan F. Fourier Transform Infrared (FTIR) Spectrometric Analysis of Structural Changes of Mushroom Polyphenol Oxidase

During Inactivation by Thermosonication. EuroFoodChem XVII. 07-10 May 2013, İstanbul, Türkiye.

Conference Paper (National)

Abstract of a paper presented at and published in the proceedings of a by an international organization

Baltacıoğlu, H., and Artık N. Trabzon Hurmasının Askorbik Asit ve Şeker Kompozisyonunun HPLC ile Belirlenmesi. 7. Gıda Mühendisliği Kongresi. 24-26 Kasım, 2011, Ankara.

Baltacıoğlu, H. Gıda Endüstrisinde Ultrason Kullanımının Enzim İnaktivasyonundaki Önemi. 3. Gıda Güvenliği Kongresi. 3-4 Mayıs, 2012, İstanbul.

Baltacıoğlu, H. Turunç Ekşisi. 3. Geleneksel Gıdalar Sempozyumu. 10-12 Mayıs, 2012, Konya.

Baltacıoğlu, H. Hasat Sonrası Depolama Boyunca Trabzon Hurması Fenolik Bileşikleri Değişimi. 11. Gıda Kongresi, 10-12 Ekim, 2012, Hatay.